Dalton Transactions

Accepted Manuscript

ROYAL SOCIETY OF CHEMISTRY

www.rsc.org/dalton

Graphical abstract

From copper(II) and the conformational flexible 3-phenylpropionate anion a series of paddle-wheel and other SBU (secondary building units) coordination polymers can be originated with rigid and flexible N-donor ligands. Magneto-structural correlations are exploited in five new compounds.

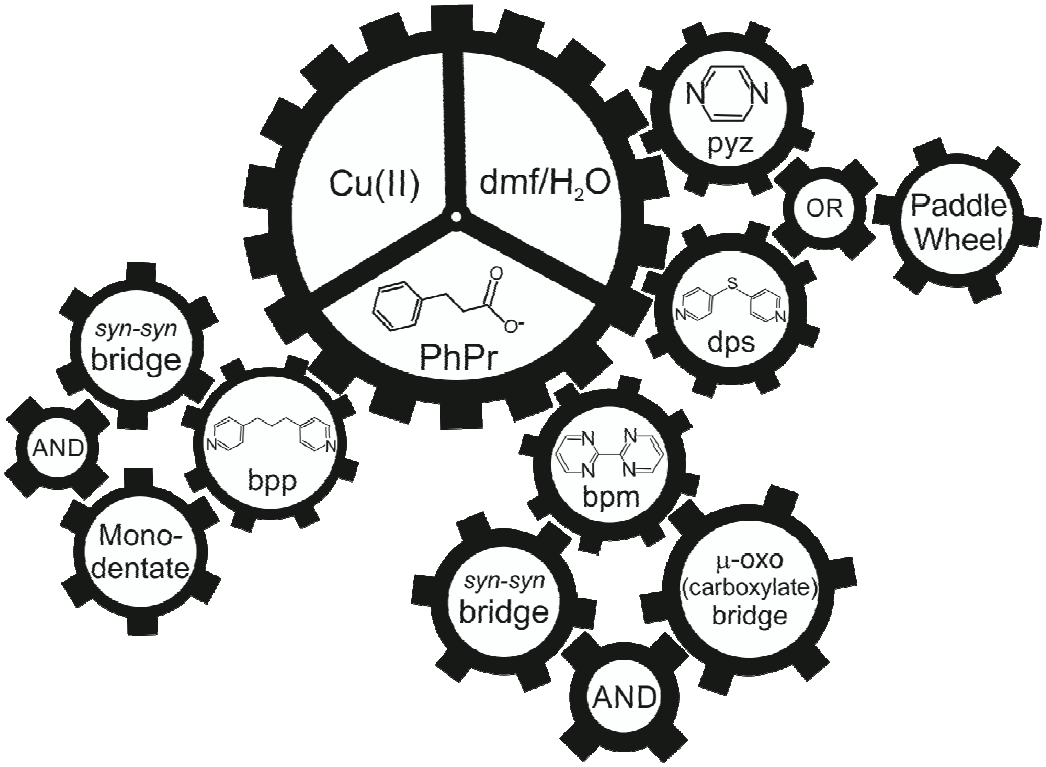

Ligand effects on the structural and magnetic versatility in a new family of one-dimensional copper(II)-3-phenylpropionate coordination polymers with *N*-donor aromatic bridging ligands

Nathália R. de Campos,[a] Marcos A. Ribeiro,[b] Willian X. C. Oliveira,[c] Daniella O. Reis,[c] Humberto O. Stumpf,*[,c] Antônio C. Doriguetto,[a] Flávia C. Machado,[d] Carlos B. Pinheiro,[e] Francesc Lloret,[f] Miguel Julve,[f] Joan Cano,[f,g] and Maria V. Marinho*[,a]

[a]*Instituto de Química, Universidade Federal de Alfenas, Campus Sede, Alfenas, MG 37130-000, Brazil. E-mail: mvmarinho09@gmail.com*

[b]*Instituto de Química, Universidade Estadual de Campinas, Laboratório de Química de Coordenação, SP 13083-970, Brazil*

[c]*Departamento de Química – ICEx, Universidade Federal de Minas Gerais, Campus Pampulha, Belo Horizonte, MG 31270-901, Brazil. E-mail: stumpf@ufmg.br*

[d]*Departamento de Química – ICE, Universidade Federal de Juiz de Fora, Campus Universitário s/n, Martelos, Juiz de Fora, MG 36036-330, Brazil*

[e]*Departamento de Física, Universidade Federal de Minas Gerais, Av Antônio Carlos, 6627, 31270-901, Belo Horizonte, MG, Brazil*

[f]*Instituto de Ciencia Molecular – Departament de Química Inorgànica, Universitat de València, C/ Catedrático José Beltrán 2, 46980 Paterna, València, Spain*

[g]*Fundació General de la Universitat de València (FGUV), Universitat de València, 46010 València, Spain*

†Electronic supplementary information (ESI) available: Experimental and calculated powder X-ray diffraction (PXRD) patterns for **1-5**, TG and DTA plots for **1-5** , crystallographic drawings of the structures of **1-5**, and theoretical calculations data for **5**. CCDC 1409932 (**1**), 1409933 (**2**), 1409934 (**3**), 1409935 (**4**), and 1409936 (**5**). For ESI and crystallographic data in CIF or other electronic format see DOI: 10.1039/x0xx00000x

Abstract

A novel series of copper(II) coordination polymers of $[Cu_2(O_2CC_8H_9)_4(pyz)]_n$ (**1**), $[Cu_2(O_2CC_8H_9)_4(dps)]_n$ (**2**), $\{[Cu(O_2CC_8H_9)_2(dps)(H_2O)]\cdot H_2O\}_n$ (**3**), $\{[NaCu(O_2CC_8H_9)_2(bpm)(NO_3)]\cdot H_2O\}_n$ (**4**), and $[Cu_4(O_2CC_8H_9)_6(OH)_2(bpp)_2]_n$ (**5**) [$O_2CC_8H_9^-$ = 3-phenylpropionate anion, pyz = pyrazine, dps = di(4-pyridyl)sulfide, bpm = 2,2'-bipyrimidine, and bpp = 1,3-bis(4-pyridyl)propane] have been synthesized and magneto-structurally investigated. Compounds **1** and **2** belong to a large group of copper(II) carboxylates where bis-monodentate pyz (**1**) and dps (**2**) ligands connect the paddle-wheel $[Cu^{II}_2(\mu\text{-}O_2CC_8H_9)_4]$ units leading to alternating copper(II) chains. The structure of **3** consists of uniform chains of *trans*-$[Cu^{II}(O_2CC_8H_9)_2]$ units linked by the bis-monodentate dps ligand. Compound **4** consists of heterobimetallic chains where $[Na^{I}_2Cu^{II}_2(\mu\text{-}O_2CC_8H_9)_4(NO_3)_2]$ units are doubly bridged by bis-bidentate bpm ligands. Compound **5** is also a chain compound whose structure is made up by tetranuclear $[Cu^{II}_4(\mu_3\text{-}OH)_2(\mu\text{-}O_2CC_8H_9)_4(O_2CC_8H_9)_2]$ units which are doubly bridged by bis-monodenate bpp ligands. The magnetic properties were investigated in the temperature range 1.8–300 K. Strong antiferromagnetic interactions across the quadruple *syn-syn* carboxylate are observed in **1** and **2** [J = –378 (**1**) and –348 cm^{-1} (**2**)] whereas a weak ferromagnetic coupling through the double out-of-plane oxo(carboxylate) bridge occurs in **4** [J = +2.66 cm^{-1}], the spin Hamiltonian being defined as $\boldsymbol{H} = -J\,\boldsymbol{S}_1 \cdot \boldsymbol{S}_2$ with $S_1 = S_2 = S_{Cu} = ½$. A quasi Curie law is observed for **3** (θ = -0.36 cm^{-1}), the bis-monodentate dps ligand being a very poor mediator of magnetic interactions. The analysis of the magnetic properties of **5** is quite complex because of the presence of two crystallographically independent tetracopper(II) units with single-μ-hydroxo, di-μ-hydroxo, μ_3-hydroxo and single-μ-hydroxo plus double *syn,syn* carboxylate bridges in each one. The nature and values of the magnetic couplings for **5** obtained by fit (intermediate, strong and weak antiferromagnetic interactions for the three former exchange pathways respectively, and intermediate ferromagnetic interactions for the latter one) were substantiated by DFT type calculations.

Introduction

The chemistry of copper(II)-carboxylate systems has been thoroughly investigated since the early 1970s[1] due to their diverse structural and specific properties.[2,3] Their use as building blocks, specially those containing dicopper(II) units in the field of molecular magnetism, has been highly rewarding.[4] The search for new carboxylate-containing oligonuclear copper(II) compounds, from di- to tri- and tetranuclear complexes, which are able to act as secondary building units (SBUs) for the construction of metal-organic frameworks (MOFs) is still a challenge field for synthetic chemists envisaging the preparation of multifunctional magnetic materials.[5]

The carboxylate group can adopt different coordination modes in its metal complexes, as illustrated in Chart 1.[2a,4,6] Among them, the *syn,syn* one has afforded a very large family of paddle wheel-type dinuclear complexes whose core consists of tetrakis(μ-carboxylato-κO:$\kappa O'$)dicopper(II) units.[6g-h] In contrast, the carboxylate complexes where the carboxylate adopts the bis-monodentate bridging mode are less common.[2a] The diversity of bridging modes of the carboxylate accounts for the different magnetic properties exhibited by its metal complexes.[6b,7] Although the copper(II) paddle-wheel complexes have been investigated for a long time, the first chain compound interlinking the paddle-wheel structure through bis-monodenate pyrazine (pyz) was described in 1974[8] and its crystalline structure reported in 2006.[9] This chain of formula $[Cu_2(pyz)(O_2CCH_3)_4]_n$ exhibits a strong antiferromagnetic coupling between the copper(II) ions through the *syn,syn*-carboxylate bridges (J ca. -345 cm^{-1}, the spin Hamiltonian being defined as $\boldsymbol{H} = -J\,\boldsymbol{S}_1\cdot\boldsymbol{S}_2$). This example shows that the combination of metal carboxylates and other coligands, either bridging or terminal, offers a straightforward preparative route to build novel MOFs.

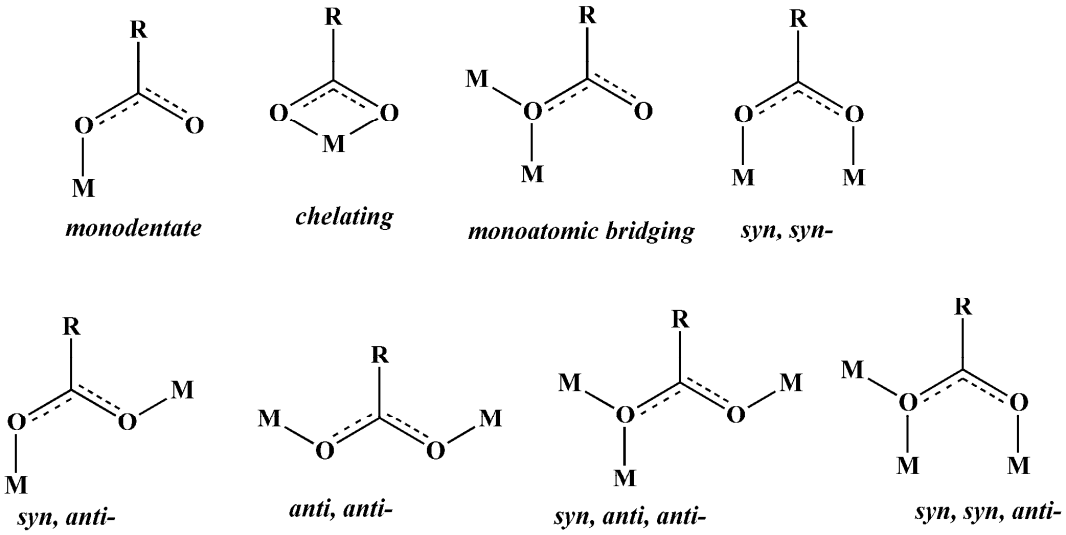

Chart 1 Coordination modes exhibited by the carboxylate ligand.

Aiming at extending the magneto-structural studies on carboxylate-containing copper(II) coordination polymers, we have chosen the 3-phenylpropionate anion also known as hydrocinnamic acid ($C_8H_9CO_2^-$ hereafter noted $Phpr^-$). This choice is based on its conformational flexibility which would allow the formation of paddle-wheel and other SBU structural motifs for the obtention of both homo- and heterometallic chains. Surprisingly, this carboxylate ligand has attracted little attention in the field of coordination chemistry, as indicated by the small number of structural reports of its metal complexes.[10] In this work, we have explored the possibility to interlink the 3-phenylpropionate-based SBUs of copper(II) through rigid and flexible nitrogen donors such as pyrazine (pyz), di(4-pyridyl)sulfide (dps), 2,2'-bipyrimidine (bpm), and 1,3-bis(4-pyridyl)propane (bpp).

We report herein the synthesis, thermal behavior, crystal structures and variable-temperature magnetic properties of five copper(II) coordination polymers of formula $[Cu_2(O_2CC_8H_9)_4(pyz)]_n$ (**1**), $[Cu_2(O_2CC_8H_9)_4(dps)]_n$ (**2**),

$\{[Cu(O_2CC_8H_9)_2(dps)(H_2O)]\cdot H_2O\}_n$ (**3**), $\{[NaCu(O_2CC_8H_9)_2(bpm)(NO_3)]\cdot H_2O\}_n$ (**4**), and $[Cu_4(O_2CC_8H_9)_6(OH)_2(bpp)_2]_n$ (**5**).

Experimental

Materials. Copper(II) nitrate trihydrate, 3-phenylpropionic acid, 2,2'-bipyrimidine (bpm), 1,3-bis(4-pyridyl)propane and *N,N*-dimethylformamide were purchased from commercial sources and used as received. Di(4-pyridyl)sulfide was prepared according to a previously reported procedure.[11] The sodium(I) salt of the 3-phenylpropionic acid of formula NaPhpr·$6H_2O$ was synthesized as follows: stoichiometric amounts of sodium hydroxide and the carboxylic acid solid were allowed to react in aqueous solution; solvent removal of the resulting clear solution in a rotary evaporator afforded the desired salt as a white solid which was filtered, washed with acetone and vacuum dried.

Preparation of Complexes. $[Cu_2(O_2CC_8H_9)_4(pyz)]_n$ (1). A dmf solution (3 mL) of pyz (33 mg, 0.41 mmol) was poured into another dmf solution (4 mL) of $Cu(NO_3)_2\cdot 3H_2O$ (100 mg, 0.41 mmol). A color change from the initial blue of the copper(II) solution to green was observed which is indicative of complex formation. Then, a dmf:water (7:2 v/v) mixture (9 mL) containing NaPhpr·$6H_2O$ (144 mg, 0.51 mmol) was slowly added. The resulting solution was set aside by one day. The small amount of a blue solid, which was not characterized, was filtered off and discarded. Several hours later, X-ray suitable green square crystals of **1** were grown in the filtered solution. They were collected, washed with cold water and dried at atmosphere for one day. Yield: 50 %. M.p.: 190 ^oC (dec). Anal. Calcd for $C_{20}H_{20}CuNO_4$ (**1**): C, 59.77; H, 5.02; N, 6.48. Found: C, 57.83; H, 4.77; N, 6.25 %. IR (KBr/cm^{-1}): 3085 (ν_{CH}), 3064 (ν_{CH}), 3026

(ν_{CH}), 2954 (ν_{CH}), 2935 (ν_{CH}), 1613 ($\nu_{CC/CN}$), 1604 (ν_{asCOO-}), 1409 (ν_{sCOO-}), 1320 ($\delta_{\delta CH}$), 1307 (δ_{CH}), and 763 ($\delta_{C\text{-}H\ out\text{-}of\text{-}plane}$).

$[Cu_2(O_2CC_8H_9)_4(dps)]_n$ (2). NaPhpr·$6H_2O$ (286 mg, 1.02 mmol) dissolved in 12 mL of a dmf:water (10:2 v/v) mixture was added to a dmf solution (6 mL) of $Cu(NO_3)_2{\cdot}3H_2O$ (200 mg, 0.82 mmol). Slow diffusion of dps ligand (154 mg, 0.82 mmol) dissolved in 6 mL of dmf was carried out and the whole was allowed to stand at room temperature. A small amount of a blue solid was also observed which was filtered off and the mother-liquor was set aside. Green parallelepipeds suitable for X-ray diffraction were grown after two days. They were collected by filtration, washed with a small amount of cold water and dried in the open air. Yield: 34 %. M.p.: 200 ^oC (dec). Anal. Calcd for $C_{46}H_{44}N_2Cu_2SO_8$ (**2**): C, 60.52; H, 4.82; N, 3.07; S, 3.50. Found: C, 60.34; H, 4.66; N, 2.94; S, 3.42 %. IR (KBr/cm^{-1}): 3088 (ν_{CH}), 3052 (ν_{CH}), 3021 (ν_{CH}), 2958 (ν_{CH}), 2931 (ν_{CH}), 1619 ($\nu_{CC/CN}$), 1608 (ν_{asCOO-}), 1411 (ν_{sCOO-}), and 717 ($\delta_{C\text{-}H\ out\text{-}of\text{-}plane}$).

$\{[Cu(O_2CC_8H_9)_2(dps)(H_2O)]\cdot H_2O\}_n$ (3). Blue needles of **3** are formed in the dmf solutions of **2** which were allowed to stand at room temperature for ten days. Yield: 50 %. M.p.: 100 ^oC (dec). Anal. Calcd for $C_{28}H_{33}N_2CuSO_6$ (**3**): C, 57.62; H, 4.63; N, 4.80; S, 5.48. Found: C, 58.15; H, 4.72; N, 4.79 %; S, 5.32. IR (KBr/cm^{-1}): 3344 (ν_{OH}), 3283 (ν_{OH}), 3095 (ν_{CH}), 3034 (ν_{CH}), 2967 (ν_{CH}), 2918 (ν_{CH}), 1618 (ν_{asCOO-}), 1590 ($\nu_{CC/CN}$), 1403 (ν_{sCOO-}), 1059 ($\delta_{C\text{-}H\ in\text{-}plane}$), 876($\delta_{CH}$), and 700 ($\delta_{C\text{-}H\ out\text{-}of\text{-}plane}$).

$\{[NaCu(O_2CC_8H_9)_2(bpm)(NO_3)]\cdot H_2O\}_n$ (4). **4** was synthesized similarly to the above complexes by using bpm (131 mg, 0.82 mmol) as nitrogen donor. X-ray suitable blue needles of **4** were grown from the solution placed in a refrigerator at 7 ºC after seven days. Yield: 40 %. Mp: 100 ^oC (dec). Anal. Calcd for $C_{26}H_{26}N_5CuNaO_8$ (**4**): C, 50.12; H, 4.21; N, 11.24 %. Found: C, 50.19; H, 3.83 and N, 10.37 %.

IR (KBr/cm^{-1}): 3463 (ν_{OH}), 3082 (ν_{CH}), 3032 (ν_{CH}), 2953 (ν_{CH}), 2909 (ν_{CH}), 1626 (ν_{asCOO-}), 1605 (ν_{asCOO-}), 1404 (ν_{sCOO-}), 1323 (ν_{sCOO-}), 1580, 1565 ($\nu_{CC/CN}$), 1385 (ν_{NO3}), 1314(ν_{NO3}), 831(ν_{NO3}), 756 ($\delta_{C\text{-}H\ out\text{-}of\text{-}plane}$), and 692 ($\delta_{C\text{-}H\ out\text{-}of\text{-}plane}$).

$[Cu_4(Phpr)_6(OH)_2(bpp)_2]_n$ (5). This compound was prepared by following an analogous procedure to that employed for **2** but replacing dps by bpp (162 mg, 0.82 mmol). Blue squares of **5** were obtained from the mother liquor on standing at room temperature after ten days. Yield: 70 %. M.p.: 140 ^{o}C (dec). Anal. Calcd for $C_{80}H_{84}N_4Cu_4O_{14}$ (**5**): C, 63.42; H, 5.54; N, 3.70. Found: C, 63.20; H, 5.48; N, 3.62 %. IR (KBr, cm^{-1}): 3443 (ν_{OH}), 3083 (ν_{CH}), 3060 (ν_{CH}), 3025 (ν_{CH}), 2926 (ν_{CH}), 1597 (ν_{asCOO-}), 1391 (ν_{sCOO-}), 1322 (ν_{sCOO-}), 753 ($\delta_{C\text{-}H\ out\text{-}of\text{-}plane}$), and 700 ($\delta_{C\text{-}H\ out\text{-}of\text{-}plane}$).

Physical Measurements. Elemental analyses (C, H, N and S) were carried out on a Perkin-Elmer 2400 analyzer. Thermogravimetry (TG) and differential thermal analysis (DTA) were performed obtained simultaneously with the same modulus employing a thermobalance (model SDT Q600, TA Instruments, USA) in the temperature range 25-1000 °C, using alumina crucibles containing samples of approximately 3 mg under a flow of N_2 (100 mL min^{-1}) at a heating rate of 10 °C min^{-1}. The TG/DTA equipment was calibrated using an indium standard for temperature and an alumina calibration weight for mass. IR spectra were recorded on a Nicolet Impact 400 spectrometer using KBr pellets in the wavenumber range of 4000-400 cm^{-1} with an average of 128 scans and 4 cm^{-1} of spectral resolution. Powder diffraction data were obtained in a powder X-ray diffractometer (model Ultima IV, Rigaku, Japan) using a CuKα tube (λ = 1.5418 Å) at a voltage of 40 kV and a current of 30 mA in the 2θ range 5-55º. Magnetic susceptibility measurements were carried out on polycrystalline samples of **1**-**5** with a Quantum Design SQUID magnetometer in the temperature range 1.9-295 K under applied dc fields of 1 T ($T \geq 100$ K) and 250 G ($T < 100$ K). The experimental magnetic

susceptibility data were corrected for diamagnetic contributions of the constituent atoms and the sample holder (a plastic bag), as well as for the temperature-independent paramagnetism (TIP) of the copper(II) ion (60×10^{-6} cm^3 mol^{-1}).

Computational Details. DFT calculations were performed on the two partially optimized geometries of the centrosymmetric and non-centrosymmetric tetracopper(II) fragments of compound **5** (see top and bottom drawings in Figure 7 and Tables S1 and S2†) through the Gaussian 09 package using the B3LYP functional,[12] the quadratic convergence approach and a guess function generated with the fragment tool of the same program.[13]Triple-ζ and double-ζ all electron basis sets proposed by Ahlrichs et al. are employed for the metal and for the rest, respectively.[14,15] The position of the hydrogen atoms from μ_3-OH groups were optimized due to their positions cannot be determined by X-ray crystallography. As it has been previously reported, the positions of these hydrogen atoms have an important influence on the magnitude of the magnetic coupling because they are directly linked to monoatomic bridges. However, the optimization of the position is not problematic because the coordination of the hydroxo group to three atoms and the possible presence of an hydrogen bond with a near carboxylate group constrain the possible conformation of the hydroxo groups.[16] The magnetic coupling states were obtained from the relative energies of the several broken-symmetry (BS) spin states from the high-spin state with parallel local spin moments. To check our results seven BS spin configuration were calculated that, for the considered different magnetic couplings, are more than the needed to evaluate the J_i constants. So, the calculated BS spin configurations and how their energies are related to the J_i magnetic coupling constants are shown in the Table S3†. Due to two occurrence of two tetracopper(II) units showing different geometries in the crystal structure of **5**, we have investigated each of them separately. To stabilize the surplus of the electronic density

on the charged external ligand, solvent effects were introduced from a polarized continuum model (PCM) with the parameters corresponding to the acetonitrile solvent that, to some extent, simulate the effect of the surrounding in the solid sate.[16,17] More details about the use of the broken-symmetry approach to evaluate the magnetic coupling constants can be found in the literature.[18a,19,20, 21]

X-ray Data Collection and Structure Refinement. X-ray diffraction data collections for **1-4** were performed with an Oxford-Diffraction GEMINI-Ultra diffractometer – LabCri, Universidade Federal de Minas Gerais – using Enhance Source Mo-Kα radiation (λ = 0.71073 Å) for **(1-3)** and Cu-*K*α radiation (λ = 1.5418 Å) for **4**. X-ray diffraction data collection for **5** was performed on Bruker D8 Venture Photon 100 diffractometer – Departamento de Química, Universidade Federal do Paraná – using graphite monochromator and Mo-Kα radiation (λ = 0.71073 Å). The values of the temperature for the data collection were 120 (**1**), 270 (**2**), 250 (**3**), 293 (**4**), and 100 K (**5**). Data integration and scaling of the reflections for compounds **1-4** were performed with the *CRYSALIS* suite.[22] Final unit cell parameters were based on the fitting of all reflections positions. Analytical absorption corrections were performed using *CRYSALIS* suite[22] and the space group identification was done with *XPREP*.[23] Data integration and reduction for compound **5** were performed using *SAINT*.[24] Data were corrected for absorption effects with *SADABS*[25] using the multi scan technique. The *XPREP* was also used in the unit cell determination. The structures of compounds **1-5** were solved by direct methods using the *SUPERFLIP*[26] program. The positions of all atoms for each compound could be unambiguously assigned on consecutive difference Fourier maps. Refinements were performed using *SHELXL*[27] based on F^2 through full-matrix least-squares routine. All non-hydrogen atoms and disordered water molecules in

3 were refined with anisotropic atomic displacement parameters. All hydrogen atoms of **1-5** (except those of the disordered water molecules in **3** which neither found nor geometrically positioned) were located in difference maps and included as fixed contributions according to the riding model.[28] The fixed parameters for the hydrogen atoms were O–H = 0.90 Å and U_{iso}(H) = 1.5 U_{eq}(O) for the water molecules, C–H = 0.97 Å and U_{iso}(H) = 1.2 U_{eq}(C) for the aromatic groups, C–H = 0.93 Å and U_{iso}(H) = 1.2 U_{eq}(C) the methylene groups and O–H = 0.93 Å and U_{iso}(H) = 1.2 U_{eq}(O) for the hydroxo ligands. A two rigid position model for all atoms, but the carboxylate group, was used to treat the disordered Phpr groups around Cu1 atom in **2** observed during the refinement process. The analysis of the structure of **4** indicated that components of the oxygen atoms ADP's along the directions of the Cu–O3 and Cu–O1 bonds are not equal in magnitude.[29] Similar results have already been reported elsewhere for complexes with the copper(II) ion in a square pyramidal environment.[30] In those cases, the metal ion has more freedom along the apical direction, since there is no coordinated atom above the basal plane, leading to ADP's for the metal atoms bigger than those of its ligand atoms. Finally, during the refinement of **2** and **3** some reflections were omitted from data [1 0 1 and 0 -1 1 (**2**) and -4 0 14 (**3**)] and they were not used in the final cycle of refinement because their intensities were significantly affected by the beam stop. The final geometric calculations were carried out with *PLATON*[31] whereas the graphical manipulations were performed with the *Mercury*[32] and *ORTEP*[33] programs. A summary of the crystal data and refinement conditions for **1-5** is given in Table 1 whereas selected bond lengths and angles for **1-5** are grouped in Table 2. The Mercury software was also used to calculate the X-ray powder diffraction patterns from both the unit cell parameters and the atomic positions obtained from the single crystal structure analysis. The X-ray diffraction patterns calculated from low temperature crystal structures (**1** and

5) are, as expected, slightly shifted (right direction) from the experimental ones performed at room temperature (298 K). Anyway, the experimental and calculated powder X-ray diffraction (PXRD) patterns (see Figures S1-S5†) regarding all five complexes, show a great coincidence of the position of all peaks expected, each pattern confirming that the obtained structure from the single crystal is equal to the one of the bulk.

Table 1. Crystallographic Data for compounds **1-5**

Complexes	**1**	**2**	**3**	**4**	**5**
Formula	$C_{20}H_{20}NO_4Cu$	$C_{46}H_{44}N_2O_8SCu_2$	$C_{28}H_{27}N_2O_6SCu$	$C_{26}H_{24}N_4NaO_8Cu$	$C_{120}H_{126}N_6O_{21}Cu_6$
Crystal size/ mm^3	0.42 × 0.30 × 0.23	0.63 × 0.24 × 0.14	0.47 × 0.16 × 0.04	0.18 × 0.12 × 0.05	0.29 × 0.24 × 0.17
Fw	401.91	911.97	583.11	621.03	2369.50
Crystal system	Monoclinic	Triclinic	Monoclinic	Triclinic	Monoclinic
Space group	C2/c	*P*$\bar{1}$	*Ia/2*	*P*$\bar{1}$	$P2_1/n$
a/ Å	17.8636 (3)	9.8067 (4)	23.9841(6)	10.024 (5)	13.3056 (15)
b/ Å	7.9173 (2)	11.9518 (5)	5.88306 (13)	10.824 (5)	18.004 (2)
c/ Å	25.9511(6)	19.7047 (7)	41.7264(13)	12.846 (5)	47.337 (5)
α/^{o}	90.00	83.844 (3)	90.00	97.185 (5)	90.00
β/°	93.810 (2)	79.762 (3)	106.501 (3)	90.782 (5)	96.278 (4)
γ/^{o}	90.00	69.662 (4)	90.00	104.175 (5)	90.00
V / $Å^3$	3662.19 (14)	2128.48 (14)	5645.1 (3)	1339.3 (10)	11272 (2)
Z	8	2	8	2	4
λ/Å	0.71073	0.71073	1.54180	0.71073	0.71073
ρ/ Mg m^{-3}	1.458	1.423	1.372	1.545	1.396
T/K	120(2)	270	250	293	100

No. parameters	235	582	344	371	1387
reflns collected	22972	19202	19345	41602	106707
reflections with $I > 2\sigma(I)$	4082	8699	4922	3535	23164
Goodness-of-fit on F^2	1.09	1.03	1.05	1.05	1.06
R^a, wR^b [$I > 2\sigma(I)$]	0.0233, 0.0544	0.0374, 0.0883	0.0743, 0.2203	0.0541, 0.1319	0.0615, 0.1522
R^a , wR^b (all data)	0.0251, 0.0554	0.0536, 0.0977	0.0818, 0.2323	0.0816, 0.1519	0.0865, 0.1654
Largest diffraction peak and hole/e A^{-3}	0.27, - 0.32	0.34, - 0.44	1.08, - 0.79	0.44, - 0.75	2.31, - 0.94

[a]$R = \sum||F_o| - |F_c||/\sum|F_o|$. [b]w$R = [\sum(|F_o|^2 - |F_c|^2)^2/\sum|F_o|^2]^{1/2}$ with $w = 1/[\sigma^2(F_o^2) + (0.0159P)^2 + 5.1699P]$ and $P = (F_o^2 + 2F_c^2)/3$ (**1**), $w = 1/[\sigma^2(F_o^2) + (0.045P)^2 + 0.6556P]$ and (**2**), $w = 1/[\sigma^2(F_o^2) + (0.1576P)^2 + 14.3824P]$ (**3**), $w = 1/[\sigma^2(F_o^2) + (0.046P)^2 + 4.4961P]$ (**4**), w $= 1/[\sigma^2(F_o^2) + (0.0729P)^2 + 30.5795P]$ (**5**) and $P = (F_o^2 + 2F_c^2)/3$ (**1-5**).

Table 2. Selected interatomic bond lengths (Å) and angles (deg) for **1-5***

		1	
Cu1—O2	1.9596(10)	O2—Cu1—O1	88.67(5)
Cu1—O1	1.9616(10)	O2—Cu1—O3	88.99 (5)
Cu1—O3	1.9644(10)	O1—Cu1—O3	169.33 (4)
Cu1—O4	1.9718 (10)	O2—Cu1—O4	169.27 (4)
Cu1—N1	2.2133 (11)	O1—Cu1—N1	94.28 (4)
Cu1—Cu1^{i}	2.6052 (3)	O2—Cu1—N1	101.81 (4)
O1—C3	1.2649 (17)	O3^{I}—C3—O1	125.82 (13)

*Symmetry code: (i) = −*x*+1/2, −*y*+3/2, −*z*+2.

		2	
Cu1—O6	1.9624(16)	O8—Cu1—O6	168.46 (7)
Cu1—O8	1.9521 (17)	O5—Cu1—O7	168.52 (7)
Cu1—O5	1.9669 (19)	O8—Cu1—O5	90.14 (10)
Cu1—O7	1.9771 (19)	O6—Cu1—O7	90.65 (9)
Cu1—N2	2.1700(19)	O8—Cu1—N2	101.21 (7)
Cu1—Cu1^{i}	2.6236 (5)	O6—Cu1—N2	90.31 (7)
O1—C10^{II}	1.255 (3)	O4^{II}—Cu2—O2	89.28 (9)
Cu2—O1	1.973 (2)	O1—Cu2—O2	88.92 (8)
Cu2—O2	1.9746 (17)	O2—Cu2—O3	89.38 (8)
Cu2—O3	1.9762 (19)	O1—Cu2—O4	89.28 (9)
Cu2—O4	1.9768 (17)	O3—Cu2—O4	90.20 (8)
Cu2—N1	2.175 (2)	O1—Cu2—N1	94.52 (8)
Cu2—Cu2^{ii}	2.6204 (6)	O2—Cu2—N1	96.97 (7)
Cu1—Cu2	10.2571(7)	O3—Cu2—N1	96.88 (8)
Cu2—Cu2^{iii}	7.7388(5)	O4—Cu2—N1	94.20 (7)
Cu1—Cu2^{iv}	9.8067(6)	O1—Cu2—N1	94.52 (8)

*Symmetry code: (i) = −*x*+2, −*y*, −*z*; (ii) = −*x*+2, −*y*+1, −*z*+1; (iii) = 1-*x*, 1-*y*, 1-*z*; (iv) = *x*, -1+*y*, *z*.

3

Cu1—O1	1.949 (3)	O2—Cu2—N1	96.95 (7)
Cu1—N1	2.032 (4)	O3—Cu2—N2	96.86 (8)
Cu2—O3	1.9766 (19)	O4—Cu2—N2	94.19 (7)
Cu2—O5	2.221 (4)	N1—Cu1—N1^{ii}	180.00 (17)
Cu2—N2	2.034 (3)	C8—S1—C3	103.6 (2)
O1—C11	1.240 (7)	O3—Cu2—O3^{i}	178.85 (17)
N1—C1	1.279 (8)	O3—Cu2—N2	89.28 (12)
		O3—Cu2—O5	90.58 (8)
		N2—Cu2—O5	93.69 (9)
		N2^{i}—Cu2—N2	172.63 (18)

*Symmetry code: (i) = −*x*+1, *y*, −*z*+1/2; (ii) = −*x*+1/2, −*y*−1/2, −*z*.

4

Cu1—O1	1.928 (2)	O1—Cu1—O3^{i}	92.30 (10)
Cu1—O3	1.972 (2)	O1—Cu1—N3	172.13 (11)
Cu1—N3	2.024 (3)	O3^{i}—Cu1—N3	93.67 (11)
Cu1—N1	2.033 (3)	O3^{i}—Cu1—N1	172.13 (11)
Na1—O2^{i}	2.267 (3)	N3—Cu1—N1	80.67 (11)
Na1—O4	2.269 (3)	O3^{i}—Cu1—O3	78.08 (10)
Na1—O6	2.416 (3)	O2^{i}—Na1—O4	88.98 (11)
Na1—O5	2.471 (3)	O4—Na1—O6	140.85 (11)
Na1—N2^{ii}	2.479 (3)	O2^{i}—Na1—O5	144.31 (12)
Na1—N4^{ii}	2.544 (3)	O4—Na1—O6	140.85 (11)
O3—C9	1.294 (4)	N2^{ii}—Na1—N4^{ii}	66.17 (10)

*Symmetry code: (i) = −*x*+1, −*y*, −*z*; (ii) = *x*+1, *y*, *z*.

5

Cu1—N1	1.993 (3)	Cu2-OH1-Cu1	111.03(12)
Cu1—O1	1.948 (3)	Cu1-OH1-Cu1^{i}	99.04 (11)
Cu1—O3	2.260 (2)	Cu2-OH1-Cu1^{i}	117.20 (13)
Cu1—OH1	1.947 (3)	Cu3-OH3-Cu4	111.46(13)
Cu1—OH1^{i}	1.982 (3)	Cu3-OH3-Cu5	116.85 (13)
Cu2—N3	1.984 (3)	Cu4-OH3-Cu5	98.37 (12)
Cu2—O2	2.264 (3)	Cu4-OH2-Cu5	98.90 (12)

Cu2—O4	1.978 (3)	Cu5-OH2-Cu6	111.03(13)
Cu2—O6	1.975 (3)	Cu6-OH2-Cu4	116.45 (14)
Cu2—OH1	1.939 (3)		
Cu3—N2	1.998 (3)		
Cu3—O7	1.977 (3)		
Cu3—O9	2.241 (3)		
Cu3—O11	1.974 (3)		
Cu3—OH3	1.940 (3)		
Cu4—N5	2.006 (3)		
Cu4—O10	1.945 (3)		
Cu4—O12	2.178 (2)		
Cu4—OH2	1.985 (3)		
Cu4—OH3	1.972 (3)		
Cu5—N4	2.002 (3)		
Cu5—O13	1.921 (3)		
Cu5—O15	2.201 (3)		
Cu5—OH2	1.959 (3)		
Cu5—OH3	1.987 (3)		
Cu6—N6	2.002 (3)		
Cu6—O14	2.269 (3)		
Cu6—O16	1.974 (3)		

*Symmetry code: (i) = $-x+1, -y+2, -z$.

Results and Discussion

Synthesis and IR Spectroscopy

Compounds **1-5** were synthesized as illustrated in Scheme 1. All of them have been obtained by diffusion in a test-shaped glass tube (1.5 cm inner diameter and 18 cm height). A unique rupture of the original lantern structure was observed when **2** was transformed into **3**. In fact, the literature describes a lantern breakdown by addition of the flexible nitrogen ligand in $\{[Cu_2(O_2CCH_2C_4H_3S)_4(bpp)_2]\}_n$ (bpp = 1,3-bis(4-

pyridyl)propane).[2a] In this work, the irreversible transformation of **2** into **3** was attributed to the instability of the paddle-wheel unit in dmf as solvent, leading to only one of the forms after ten days in solution at room temperature.

We have used the same solvent, room temperature and molar ratio of the reactants for all complexes, except for **4** where the temperature of crystallization was adjusted. In this case, it is worth noting that the temperature of the crystallization and the bpm ligand were crucial in **4** since the solvent and the ratio of the 3-phenylpropionate anion with copper(II) ions were similar to those of the other four complexes. Recently, the literature reported the preparation of related heterobimetallic sodium(I)/cobalt(II)-formate coordination polymers by adjusting the solvent and ratio of the reactants via solvothermal synthesis.[34]

The most relevant aspect for the IR spectra of **1-5** concerns the values of asymmetric and symmetric stretching frequencies of the carboxylate groups of the phenylpropionate ligand (see Figure S6). The frequency difference (Δ) between ν_{asym}(COO) and ν_{sym}(COO) stretches in the carboxylate-containing complexes in comparison to the corresponding values in ionic species is currently taken as diagnostic of the coordination mode of the carboxylate group.[2a,35] The $\nu_{asym}(COO^-)$ and $\nu_{sym}(COO^-)$ vibrations of the 3-phenylpropionate for **1** and **2** occur at 1604 and 1409 cm^{-1} (Δ = 195 cm^{-1}, **1**) and 1608 and 1411 cm^{-1} (Δ = 197 cm^{-1}, **2**) whereas those of the sodium salt of the 3-phenylproprionate are 1551 and 1350 cm^{-1} (Δ = 201 cm^{-1}). These results indicate that the carboxylate groups in **1** and **2** coordinate to the copper(II) ions in a symmetrically *syn-syn* bridging mode. Δ for **3** is equal to 215 cm^{-1}, a value which suggests a monodentate coordination of the carboxylate for this compound. The occurrence of two (**4**)/one (**5**) $\nu_{asym}(COO^-)$ [1626 and 1605 cm^{-1} (**4**) and 1597 cm^{-1} (**5**)] and two (**4**/**5**) $\nu_{sym}(COO^-)$ [1404 and 1323 cm^{-1} (**4**) and 1391 and 1322 cm^{-1} (**5**)] point

out the presence of two different coordination modes of the carboxylate groups in **4** and **5**. About the ν(CC/CN) stretching frequencies of the pyz, dps, bpm and bpp the infrared spectra show peaks at 1623 (**1**), 1619 (**2**), 1590 (**3**), 1580, 1565 (**4**), and 1603 cm^{-1} (**5**). These values are consistent with their coordination to copper(II) as bridges via the pyridyl-nitrogen atoms.[2a,11,36] Finally, peaks at 1385 and 831 cm^{-1} in the spectrum of **4** are due to the presence of the nitrate ion.[37] All these spectroscopic features for **1**-**5** have been confirmed by their X-ray structures (see below).

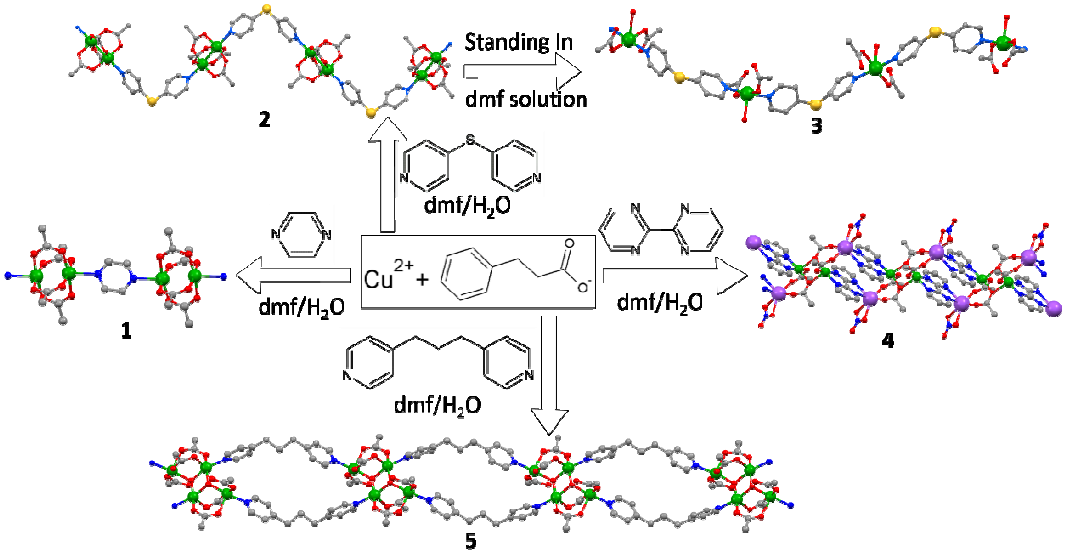

Scheme 1. General synthetic route to 3-phenylpropionate-containing copper(II) coordination polymers using the pyz (**1**), dps (**2** and **3**), bpm (**4**) and bpp (**5**) *N*-donors as spacers.

Thermal Study. Thermogravimetric curves of **1**–**5** are shown in Figure S7A†. The TG curves of compounds **1** and **2** reveal that they are stable up to 155 and 196 ^{o}C respectively, in agreement with the absence of solvent molecules in their structures. Two steps of weight loss in the temperature ranges 155-215 and 245-325 ^{o}C occur in **1**. The first one corresponds to the release of one pyrazine molecule (obsd. 10.2%; calcd. 10.0%) whereas the second one is attributed to the decomposition of the 3-

phenylpropionate ligands. The remaining mass at 355 ^{o}C, agrees with a mixture of CuO and $CuCO_3$ that slowly decomposes releasing CO_2 and affording a residue at 700 ^{o}C, mass that would correspond to CuO (obsd. 19.5%, calcd. 19.8%).[2a] For the compound **2**, the first weight loss occurs abruptly in the temperature range 200-350 ^{o}C and it would correspond to the decomposition of the di(4-pyridyl)sulfide and 3-phenylpropionate ligands (obsd. 73.6 %, calcd. 72.9 %). The residue at 355 ^{o}C which is identified as $CuCO_3$ (obsd. 26.2 %, calcd. 27.1 %) undergoes a slow decomposition by releasing CO_2 at higher temperatures and it transforms into CuO at 800 ^{o}C (obsd: 18.3 %, calcd. 17.5 %). The TG curve for **3** shows a first weight loss in the temperature range 78-107 ^{o}C corresponding to two water molecules (obsd: 6.2 %, calcd. 6.17 %). Afterwards, the decomposition of the organic moiety takes place in more than one step, which are difficult to identify. The final residue at 800 ^{o}C (ca. 18.7 %) would be CuO (13.6 %) associated with some carbonized material. In the case of **4**, the TG curve presents a gentle decline up to 200 ^{o}C, corresponding to the release of one water molecule (obsd 3.1 %, calcd. 2.9 %). Afterwards, the decomposition occurs in at least four steps and at 800 ^{o}C the residue is consistent with CuO + ½ Na_2O (obsd. 17.8 %, calcd. 17.8 %). The TG curve for **5** shows various steps of decomposition starting at low temperature (ca. 40 ^{o}C) and the organic moiety is almost totally decomposed at 400 ^{o}C, the remaining solid at this temperature being practically $CuCO_3$ (obsd. 36.2 %, calcd. 31.3 %). It further decomposes slowly releasing CO_2 and the residue at 750 ^{o}C is identified as CuO (obsd: 19.2 %, calcd. 20.1 %).

All these thermal decompositions are in agreement with the DTA behaviors (Figure S7B†). As an illustrative example, one endothermic peak is observed in the DTA curve of **4** at 190 °C which is due to the removal of one water molecule and the other peaks at 267 and 326 ^{o}C are attributed to the decomposition process of this complex.

Description of the Structures. $[Cu_2(O_2CC_8H_9)_4(pyz)]_n$ (1) and $[Cu_2(O_2CC_8H_9)_4(dps)]_n$ (2). The crystal structures of **1** and **2** consist of neutral centrosymmetric paddle-wheel dinuclear copper(II) units, $[Cu^{II}_2(\mu\text{-}O_2CC_8H_9)_4]$, which are further connected by pyz (**1**) and dps (**2**) bridging ligands to give linear or waving chains, respectively (Figures 1–3).

Each copper(II) ion in **1** (Cu1) and **2** (Cu1 and Cu2) is five-coordinate in a somewhat distorted square pyramidal surrounding. Four carboxylate-oxygen atoms from four 3-phenylpropionate ligands build the basal plane at the copper atom (**1**/**2**) whereas a nitrogen atom from the pyz (**1**)/dps (**2**) occupies the apical site. The values for the trigonality parameter τ[38] are 0.001 for Cu1 in **1** and 0.001 and 0.004 for Cu1 and Cu2 in **2**. The copper(II) ions are shifted from the mean basal plane by 0.1823(5) Å (**1**), and 0.1940(10) (Cu1) and 0.1965(9) Å(Cu2) (**2**) toward the apical position.

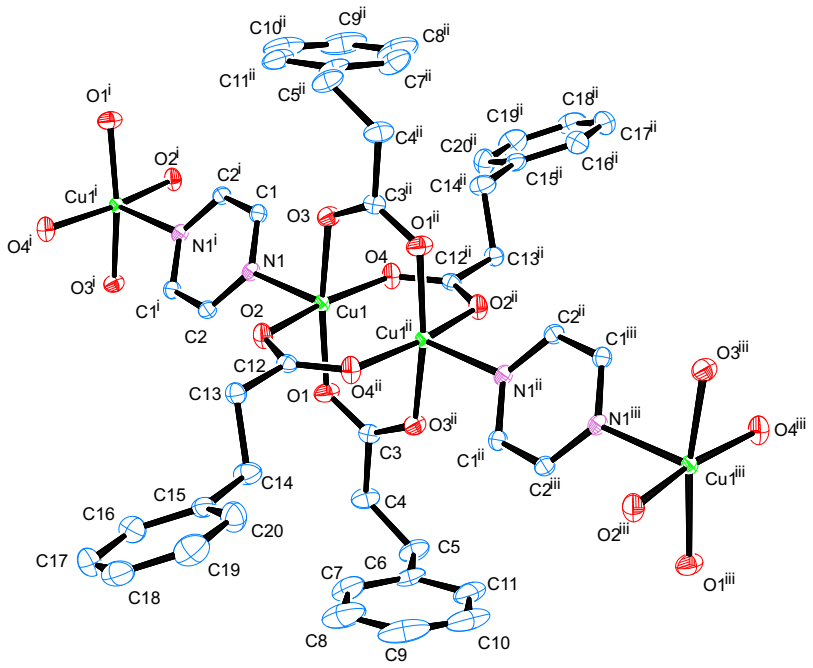

Figure 1. Perspective view of a fragment of the structure of **1** with the atom numbering scheme. Hydrogen atoms are omitted for the sake of clarity [Symmetry codes: (i) = 1-*x*, 1-*y*, 2-*z*; (ii) = 1/2-*x*, 3/2-*y*, 2-*z*; (iii) = -1/2+*x*, 1/2+*y*, *z*].

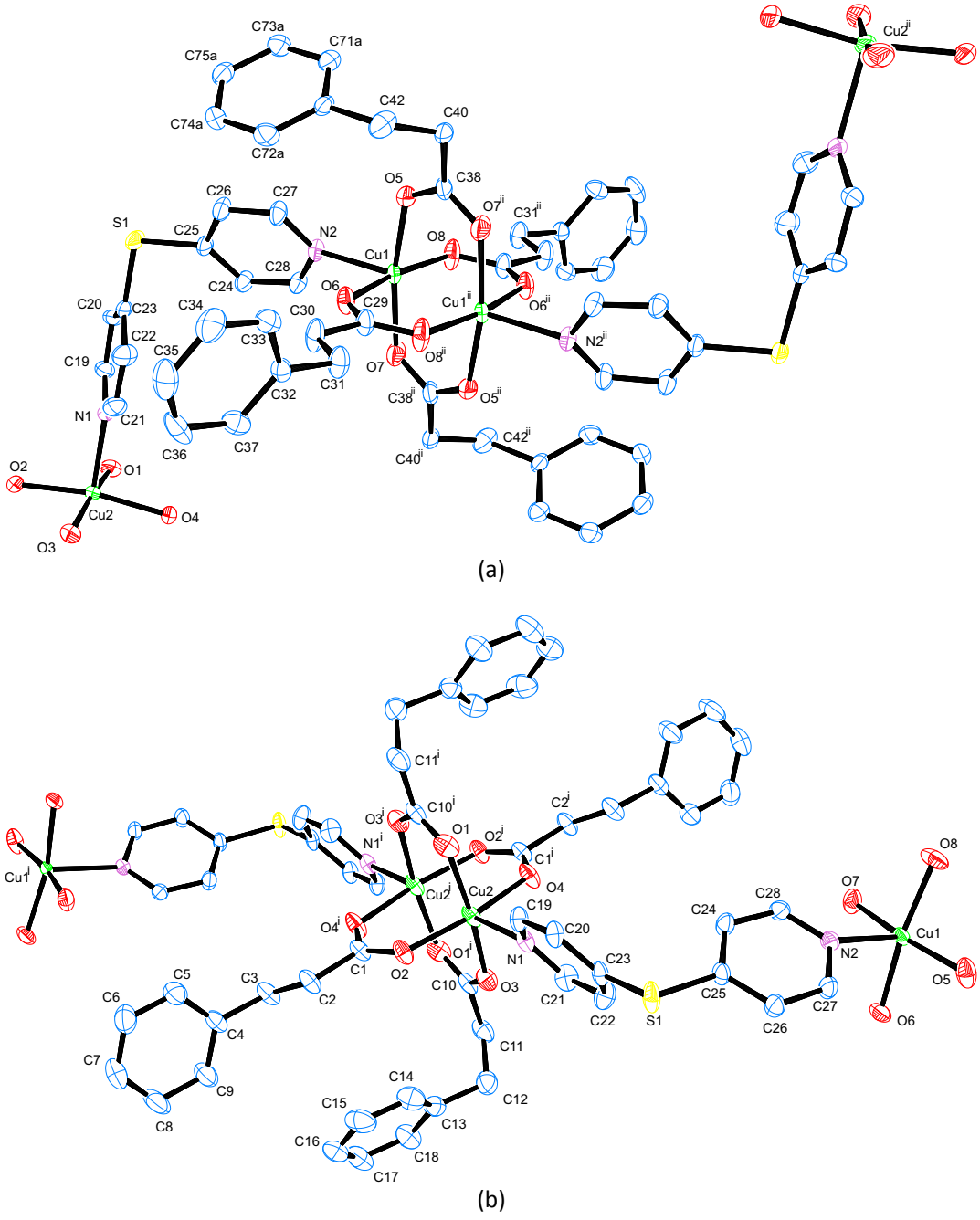

Figure 2. Perspective views of the two centrosymmetric fragments in the structure of **2** with the atom numbering scheme. Hydrogen atoms are omitted for the sake of clarity [Symmetry codes: (i) = -*x*+2, -y+1, -z+1; (ii) = -*x*+2, -*y*, -*z*].

The 3-phenylpropionate ligand in **1** and **2** adopts the *syn,syn*-(μ-O,O') coordinative mode between the copper(II) ions forming a paddle-wheel with basal Cu-O distances varying in the ranges 1.9596(10) - 1.9718(10) (**1**) and 1.9521(17) - 1.9771(19) Å (**2**) (Figure S8). These distances are smaller than the apical Cu–N ones [2.213(1) and 2.170(2)/2.175(2) Å for **1** and **2**, respectively]. The copper-copper separations within each carboxylate-bridged dicopper(II) unit are 2.6052(3) Å (Cu1···Cu1^{i}) (**1**) and 2.6236(5) (Cu1···Cu1^{ii})/2.6204(6) Å (Cu2···Cu2^{ii}) (**2**), as previously reported for Cu(II) paddle-wheel complexes.[6c]

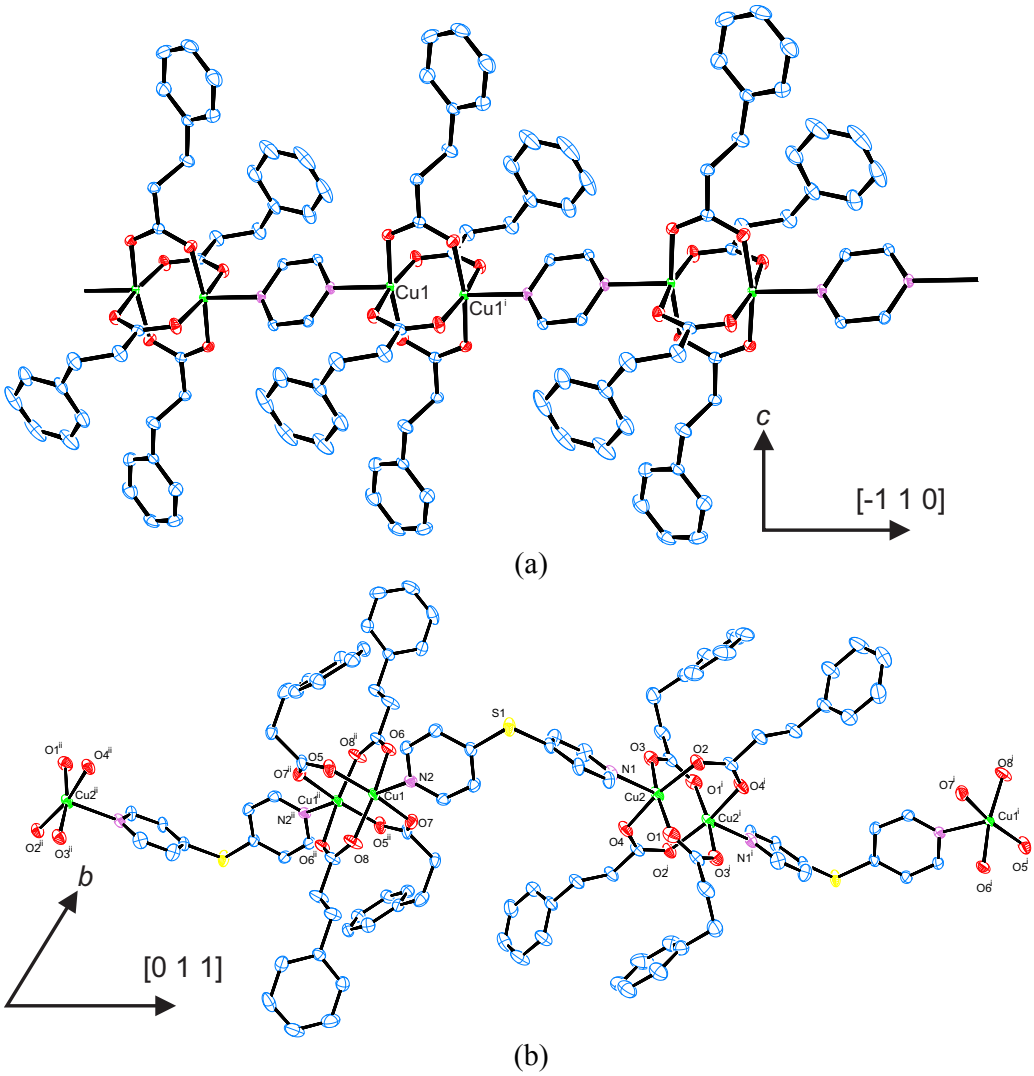

Figure 3. View of a fragment of the chains of **1** (a) and **2** (b) growing along the [-110] and [110] directions, respectively.

The paddle-wheel $[Cu^{II}_2(\mu\text{-}O_2CC_8H_9)_4]$ units of **1** and **2** are connected by pyz and dps bridges respectively leading to neutral chains that grow along the [-110] and [110] directions (Figure 3). The values of the copper-copper distance through the bis-monodentate pyz (**1**) and dps (**2**) ligands are 7.2021(2) Å ($Cu1\cdots Cu1^{ii}$) and 10.2571(7) Å (Cu1···Cu2). The chains of **1** extend into 2D networks parallel to the (001) and (002) planes through intermolecular interactions involving a carboxylate oxygen (O2) atom and a hydrogen atom of a propyl CH_2 group from the adjacent chain with a O2···C18 distance of 3.272(2) Å (Figure S9†). A supramolecular 2D structure also occurs in **2** (Figure S10†), the chains being interlinked by weak C–H···O type and C-H···S type interactions [O2···C20 and S1···C11 distances are of 3.461(3) and 3.783(3) Å, respectively] along the [011] direction.

$\{[Cu(O_2CC_8H_9)_2(dps)(H_2O]\cdot H_2O\}_n$ (3). Unlike the paddle-wheel chain structure in **2**, the crystal structure of **3** is made up of di(4-pyridyl)sulfide-bridged wavy polymeric chains of neutral copper(II) units $[Cu^{II}(\mu\text{-}O_2CC_8H_9)_2]$ which grow along the crystallographic *c* axis (Figure 4). The two crystallographically independent copper(II) ions in **3** (Cu1 and Cu2) exhibit the same five-coordinate CuN_2O_3 environment. Two 3-phenylpropionate-oxygen atoms [O1 and $O1^{ii}$; (ii) = 1/2-*x*, *y*, 1-*z*] and two nitrogen-atoms (N1 and $N1^{ii}$) from two dps molecules build the basal plane at Cu1, the apical position being filled by a water molecule (O5). The bond distances in the distorted square-pyramidal geometry environment around Cu1 (τ = 0.1) are Cu1–O1 = 1.949(3), Cu1–N1 = 2.032(3) Å, and Cu1–O5 = 2.217(4) Å (Figure S11b). In the case of Cu2, two oxygen atoms [O3 and $O3^{i}$, (i) = 1/2-*x*, 1/2-*y*, 1/2-*z*] from the 3-phenylpropionate ligands, two nitrogen atoms (N2 and $N2^{i}$) from two dps molecules build the basal plane and one disordered oxygen atom (O6 and $O6^{i}$) of a water molecule fills the apical

position, the whole resulting in a perfect square-pyramidal geometry. This copper atom is placed in an inversion center and due to this special position, it exhibits two possibilities of coordination of the water molecule, which led us to fix the occupancy of the water oxygen atom O6 as 0.5 in order to have its anisotropic displacement parameter similar in magnitude of the other atoms in its environment (the thermal analysis for **3** supports the amount of water and indirectly this conclusion). Considering the environment of Cu2, the pattern of two shorter equatorial distances [Cu2-O3 = 1.947(3) and Cu2–N2 = 2.029(4) Å] compared to the axial one [Cu2–O6 = 2.64(1) Å] is as expected due to the Jahn-Teller effect for copper(II) ion. The long Cu2–O4 distance [Cu2–O4= 2.751(4) Å] allows to assume that the 3-phenylpropionate anions act as a monodentate ligand versus Cu2 (Figure S11a).

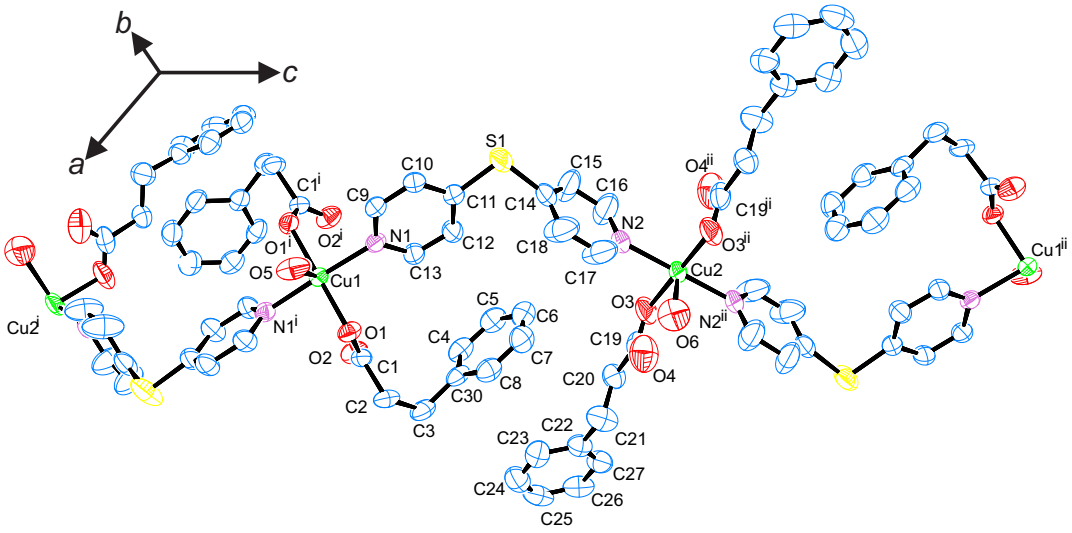

Figure 4. View of a fragment of the chain of **3** showing the coordination environment for the copper(II) atoms with the atomic numbering scheme. Hydrogen atoms have been omitted for clarity.

The distinct structures of **2** and **3** can be also evidenced in the intrachain copper···copper distances. The four 3-phenylpropionate groups in **2** adopt symmetric *syn-syn* carboxylate bridging modes building paddle-wheel dicopper(II) units with a Cu···Cu distance of 2.6237(5) Å, while the 3-phenylpropionate anions in **3** act as monodentate ligands and the dps molecule links the copper(II) centers, the intrachain Cu1···Cu2 distance in **3** being 10.9632(4) Å.

The polymeric chains of **3** are interlinked along the crystallographic *b* axis by hydrogen bonds involving the non-coordinated oxygen atoms of 3-phenylpropionate (O4 and O2) and the coordinated water molecules (O5 and O6). The former and latter act as hydrogen bond acceptor and donor, respectively (Figure S12). These weak intermolecular interactions lead to a two-dimensional supramolecular structure parallel to the (100) plane. One of the hydrogen atoms of the water molecule O6 is hydrogen bonded to the non-coordinated oxygen (O4) from the 3-phenylpropionate anion (Figure S12). The interconnection between parallel chains along the crystallographic *b* axis results in the shortest metal-metal separation [Cu1–Cu1 = Cu2–Cu2 = *b* axis dimension = 5.883(1) Å] for **3** (Figure S13a). The uncoordinated disordered water molecules, which fill the channel along the [010] direction, contribute to stabilize the whole packing structure via hydrogen bonding (Figure S13b)

$\{[NaCu(O_2CC_8H_9)_2(bpm)(NO_3)]\cdot H_2O\}_n$ (4). The crystal structure of **4** consists of heterobimetallic double chains built up by centrosymmetric tetranuclear sodium(I)-copper(II) units, $[Na^{I}_2Cu^{II}_2(\mu\text{-}O_2CC_8H_9)_4]$, which are further connected by two 2,2'-bipirimidine molecules acting as bis-bidentate ligands between the Na^{I} and Cu^{II} ions of adjacent units (Figures 5 and 6).

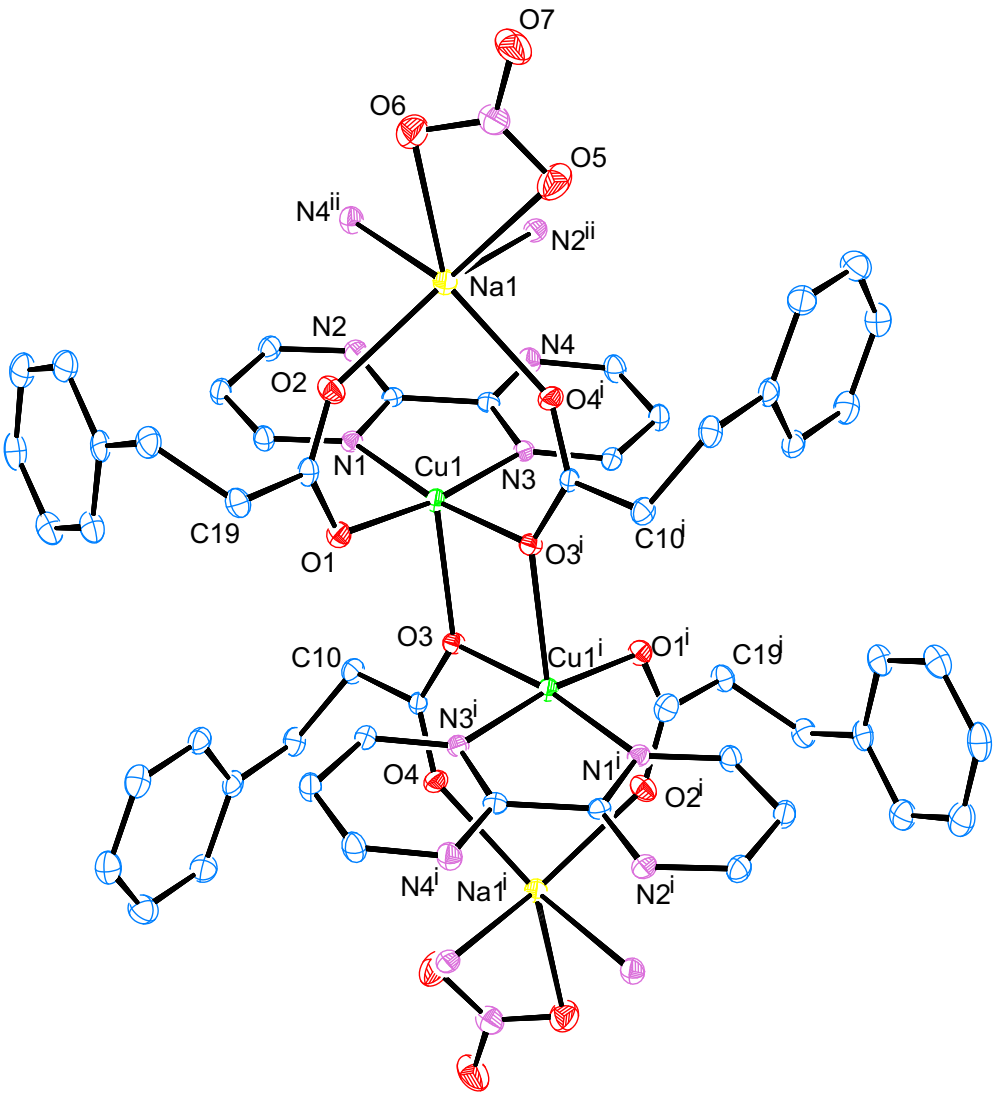

Figure 5. Perspective view of the centrosymmetric tetranuclear unit in **4** with the atom numbering scheme. Thermal ellipsoids are shown at the 50% probability level. Hydrogen atoms were omitted for clarity.

Each Cu(II) ion in **4** is five-coordinate with three carboxylate-oxygen atoms (O1, O3 and O3^{i}) of the 3-phenylpropionate groups and two nitrogen atoms (N1 and N3) of the bpm molecule in a slightly distorted square pyramidal environment ($\tau = 0.0008$). The basal plane is formed by the N1, N2, O1 and O3^{i} [symmetry code: (i) = 1–*x*, –*y*,–*z*] atoms and the apical position is occupied by the symmetry related O3 atom (Figure 5).

The basal Cu1–O and Cu1–N distances [Cu1–O1 = 1.928(2), Cu1–O3^{i} = 1.972(2), Cu1–N1 = 2.033(3), and Cu1–N3 = 2.024(3) Å] are in agreement with the values found in **1** and **2** and those from the literature.[39] The apical Cu1–O3 distance of 2.276(3) Å is significantly longer than the equatorial ones. The angle subtended at the Cu1 atom by the bpm ligand is 80.67(1)º. The remaining oxygen atoms of the carboxylate ligands [O2 and O4^{i} ; (i) = 1–*x*, –*y*,–*z*] and two nitrogen atoms of the bpm molecule [N2^{ii} and N4^{ii} (ii) = -*x*, -*y*, -*z*] build the equatorial plane at the Na1 atom [least-square plane r.m.s. deviation = 0.0914(16) Å]. The sodium atom is shifted by 0.3590(36) Å from this mean plane. The six-coordination around Na1 is completed by the O5 and O6 oxygen atoms from a chelating nitrate anion leading to a *cis*-NaO_4N_2 distorted octahedral environment (Figure S14). The Na1–O and Na1–N bond lengths [Na1–O4^{i} = 2.271(3); Na1–O2 = 2.267(3); Na1–O6 = 2.418(4); Na1–O5 = 2.471(4); Na1–N2^{ii} = 2.479(4) and Na1–N4^{ii} = 2.545(4) Å; symmetry codes: (i) = 1-x, -*y*, -*z* and (ii) = -*x*, -*y*, -*z*] are in agreement with those ones previously found other Na(I) complexes.[36,40] The bridging bpm ligand is planar (r.m.s deviation of fitted atoms = 0.012 Å) and its bond distances and angles are as expected.

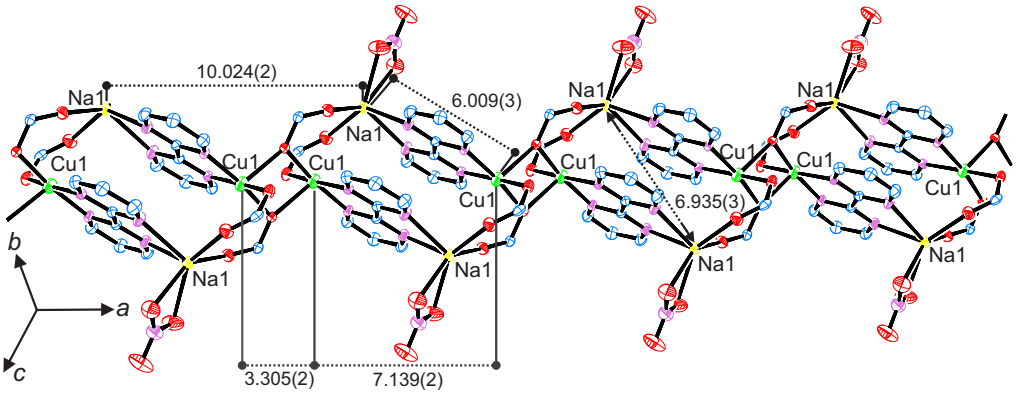

Figure 6. Projection view onto the plane (014) of a fragment of the double chain in **4** which grows parallel to the crystallographic *a* axis. Hydrogen atoms were omitted for clarity.

Each pair of 3-phenylpropionate bridging ligands within the tetranuclear $[Na^{I}_2Cu^{II}_2(\mu\text{-}O_2CC_8H_9)_4]$ units, act in an asymmetric *syn,syn,anti*-(μ-O,O') coordination mode toward the two Cu^{II} and one Na^{I} ions, with one short and one long Cu-O distance (Figure 5). The Na^{I} and Cu^{II} ions from adjacent $[Na^{I}_2Cu^{II}_2(\mu\text{-}O_2CC_8H_9)_4]$ units are further bridged by two bis-bidentate bpm molecules affording $Cu^{II}_2Na^{I}_2$ cages that alternate regularly along the double sodium(I)-copper(II) chains (Figure S15). This metallacyclic cage has a cavity with a diameter of 7.139(4) and 6.935(3) Å, considering the distances between directly opposed copper and sodium atoms, respectively. It is interesting to note that in the $Cu^{II}_2Na^{I}_2$ motif the four 3-phenylpropionate bridging ligands are oriented with their phenyl rings toward the ring center, working as a cage gate. The opposing rings are separated by *ca.* 13 Å and the two pairs of phenyl rings are slightly shifted "upward" and "downward" (see Figure S15).

It is interesting to note that within the Cu_2O_2 motif each bridging oxygen (O3 and $O3^{i}$) simultaneously occupies an apical site at one Cu^{II} ion and the basal position of the other Cu^{II} ion (see Figure 5], the apical Cu1-O3 distance [2.276(4) Å] being longer than the basal Cu1-$O3^{i}$ bond length [1.972(3)]. This is a typical structural aspect for parallel-planar dinuclear Cu^{II} complexes with two oxo(carboxylate) bridges.[2a] Thus, the Phpr ligands act as monoatomic bridges through of the oxygen atom (O3) linking individual cages and leading to a 1D polymer which grow parallel to the crystallographic *a* axis (Figure 6). The copper-copper separation through the double oxo(carboxylate) bridge and the value of the angle at the oxo(carboxylate) atom are 3.305(2) Å and 101.93(9)º, respectively. The values of the intrachain copper-sodium distances are 3.663(1) (Cu1···Na1) and 6.009(3) Å [Cu1···$Na1^{iii}$; symmetry code: (iii) = -1+*x*, *y*, *z*].

The double chains in **4** are cross-linked by means of weak supramolecular interactions involving C-$H_{aromatic}$ and nitrate-oxygen atoms, the main contacts occurring along the crystallographic *b* and *c* axes (Figure S16).

$[Cu_4(O_2CC_8H_9)_6(OH)_2(bpp)_2]$ (5). The crystal structure of **5** consists of double chains built up by centrosymmetric and non-centrosymmetric tetranuclear copper(II) units, $[Cu^{II}_4(\mu_3\text{-}OH)_2(\mu\text{-}O_2CC_8H_9)_4(O_2CC_8H_9)_2]$, which are further connected by two 1,3-bis(4-pyridyl)propane molecules acting as bis-monodentate ligands between the inner and outer Cu^{II} ions of adjacent units (Figure 7). The resulting neutral chains run along the crystallographic *c* axis (Figure 8).

The two tetracopper(II) fragments in **5** have very similar structures from a topological point of view: two μ_3-hydroxo groups connect the four copper(II) ions, each one connecting the two inner copper centers [Cu1 and Cu^i (unit 1) and Cu4 and Cu5 (unit 2)] and an outer one [Cu2 and $Cu2^i$ (unit 1) and Cu3 and Cu6 (unit 2)]. Additionally, each outer copper(II) ion is linked to an inner one through two *syn,syn*-(μ-O,O') carboxylate groups from the 3-phenylpropionate ligands with one short and one long Cu-O distance (Figure 7). Each outer copper(II) ion has a monodentate Phpr ligand in its coordination sphere. In fact, the main difference comparing the two tetranuclear units concerns the conformation/orientation of the 3-phenylpropionate anions (Figure 8a). This feature is most likely responsible for the unit cell volume duplication observed in **5**.

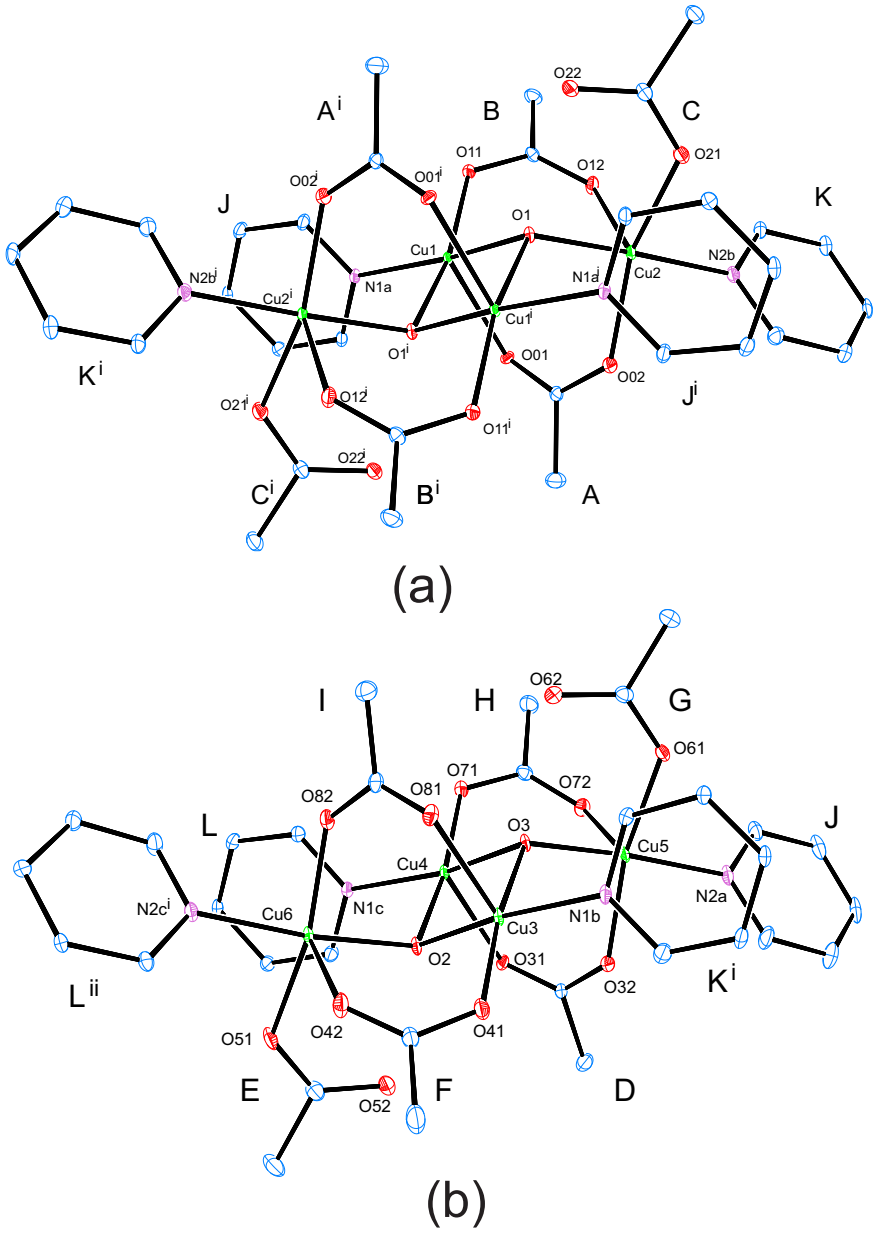

Figure 7. Perspective views of the centrosymmetric (a) and non-centrosymmetric (b) tetranuclear units in **5** with the atom numbering scheme. Hydrogen atoms are omitted for clarity [Symmetry code: (i) = 1-*x*, 2-*y*, -*z*; (ii) = -*x*, 2-*y*, 1-*z*]. K, J and L denote the different bpp ligands in **5**.

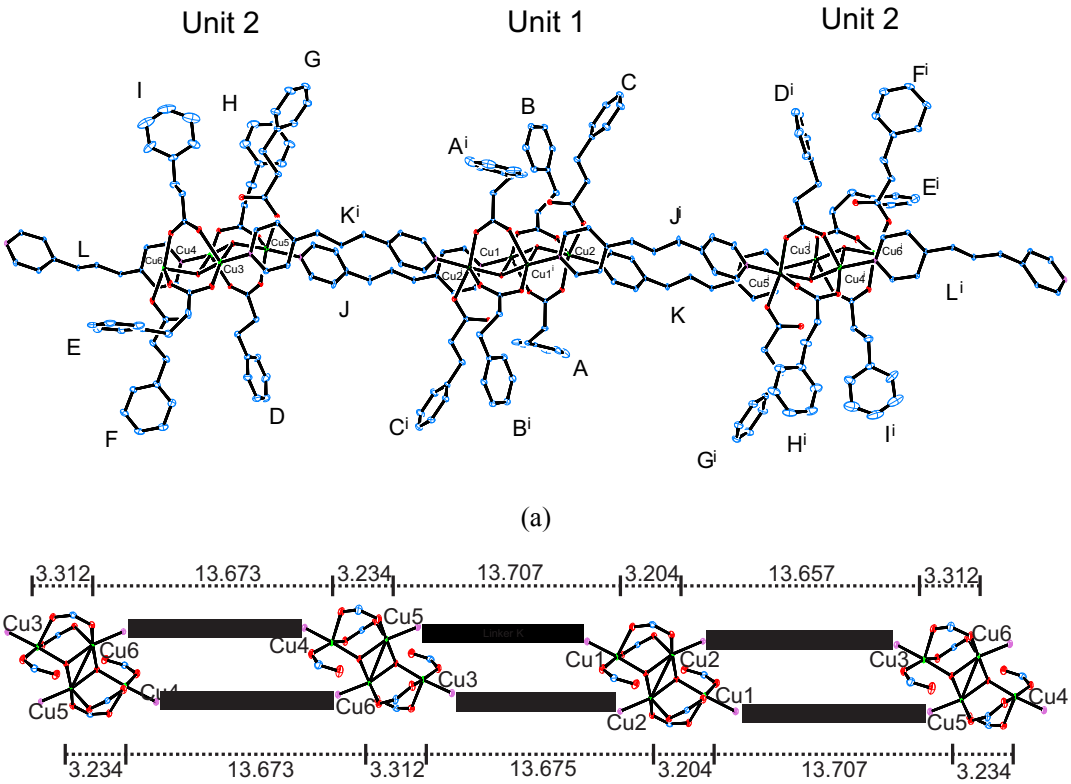

Figure 8. (a) View of a fragment of the double chain in **5** showing the regular alternation of centrosymmetric (unit 1) and non-centrosymmetric (unit 2) tetranuclear units. (b) Schematic view of a sequence of tetranuclear units connected by the bpp molecules which act as bridges. The main intrachain copper-copper separations are also shown.

All the copper(II) ions in **5** are five-coordinate in distorted square pyramidal environments [values of τ equal to 0.04 (Cu1), 0.3 (Cu2), 0.06 (Cu3), 0.05 (Cu4), 0.1 (Cu5) and 0.2 (Cu6)] with very similar bond distances and interbond angles. The basal planes of the outer Cu2 and Cu2^{i} (unit 1) and Cu3 and Cu6 (unit 2) atoms are comprised by one oxygen atom of the *syn,syn* carboxylate(3-phenylpropionate) ligands (O4, O13, and O16 for Cu2, Cu3, and Cu6, respectively), one oxygen atom of the monodentate 3-phenylpropionate ligands (O6, O7, and O17 for Cu2, Cu3, and Cu6, respectively), one

oxygen atom of the hydroxo bridges ligands (OH1, OH3, and OH2 for Cu2, Cu3, and Cu6, respectively) and one nitrogen atom of the bpp ligands (N3, N4, and N6 for Cu2, Cu3, and Cu6, respectively) (Figure 7). The basal planes of the inner Cu1 and $Cu1^{i}$ (unit 1) and Cu4 and Cu5 (unit 2) atoms are constituted by one oxygen atom of the 3-phenylpropionate ligands (O1, O7, and O10 for Cu1, Cu3, and Cu4, respectively), two oxygen atoms from the hydroxo bridges (OH1 and $OH1^{i}$ for Cu1 and $Cu1^{i}$ and OH2 and OH3 for Cu4 and Cu5), and one nitrogen atom of the bpp ligands (N1, N2, and N5 for Cu1, Cu3, and Cu4, respectively) (Figure 7). An oxygen atom of the 3-phenylpropionate ligands (O3, O2, O9, O12, O15, and O14 for Cu1, Cu2, Cu3, Cu4, Cu5, and Cu6, respectively) occupies the apical position completing the coordination environment (Figure 7). The mean value of the apical Cu-O bond distance [2.24(4) Å] is significantly longer than the mean equatorial one [1.96(2) and 1.99(1) Å for Cu-O and Cu-N, respectively].

It is interesting to note that each hydroxide ion within the units 1 and 2 connects three copper(II) ions with values at the hydroxo bridge covering the ranges 99.04(11)-117.20º (unit 1) and 98.37(12)-116.85(13)º (unit 2). The values of the copper-copper separation within the units 1 and 2 are: 2.9888(7) [$Cu1\cdots Cu1^{i}$], 3.347(1) [$Cu1^{i}\cdots Cu2$], 3.204(1), [Cu1···Cu2], 2.9970(7) [Cu4···Cu5], 3.347(1) [Cu3···Cu5], 3.335(1) [Cu4···Cu6], 3.233(1) [Cu3···Cu4], and 3.212(1) Å [Cu5···Cu6].

As can be seen in Figure 8a, the highly flexible bpp ligands adopt a *trans-trans* conformation with respect to the relative orientations of the CH_2 groups providing larger nitrogen to nitrogen separations and consequently higher periodic wavelengths. The bpp molecules cooperate each other by adjusting their coordinations and conformations to result in a neutral chain of tetracopper(II) units propagated along the [101] direction (Figures 8 and Figure S17. The copper-copper separation through the bpp bridges vary

in the range 11.791 -13.707 Å. The chains are stacked parallel to the planes (020) and (101) and they are separated by 9.003 and 12.385 Å (Bragg´s law distances), respectively. The shortest copper-copper separation between tetracopper(II) units of adjacent chains cover the narrow range 8.322-8.460 Å and it concerns parallel double chains along crystallographic *b* axis (Figure S18).

Magnetic Properties. The magnetic properties of **1** and **2** in the form of the χ_M *vs*. *T* plots [χ_M being the molar magnetic susceptibility per dicopper(II) unit] are shown in Figure 9. At room temperature, the values of $\chi_M T$ are 0.38 (**1**) and 0.46 $cm^3\ mol^{-1}\ K$ (**2**). They are well below the expected one for two magnetically isolated copper(II) ions [$\chi_M T = (2N\beta^2 g^2/3k_B)S_{Cu}(S_{Cu} + 1) = 0.83\ cm^3\ mol^{-1}\ K$ with $S_{Cu} = ½$ and $g = 2.1$]. Upon cooling, χ_M and $\chi_M T$ decrease continuously from room temperature and they vanish around 50 K for both **1** and **2**. χ_M exhibits a broad maximum above room temperature. This magnetic behavior of **1** and **2** supports the occurrence of ground singlet spin state (S = 0) resulting from strong antiferromagnetic coupling between the two copper(II) ions through the four *syn-syn* carboxylate bridges within the paddle-wheel dicopper(II) entity.

From the structural point of view, these paddle-wheel dicopper(II) units in **1** and **2** are interlinked by pyz (**1**) and dps (**2**) molecules into chains alternating chains. However, from a magnetic point of view, these systems can be viewed as dinuclear entities of $Cu^{II}_2(carboxylate)_4$ because of the negligible exchange coupling through the long Cu^{II}-(μ-pyz)-Cu^{II} (ca. 7.20 Å) and Cu^{II}-(μ-dps)-Cu^{II} (ca. 10.26 Å) pathways. Thus, the magnetic data of both complexes were analyzed through the simple Bleaney-Bowers expression [eq (1)]

$$\chi_M = (2N\beta^2 g^2/kT)/[3 + \exp(-J/kT)] \qquad (1)$$

derived through the isotropic spin Hamiltonian $\mathbf{H} = -J\,\mathbf{S_1}\cdot\mathbf{S_2} + g\beta\mathrm{H}(\mathbf{S_1} + \mathbf{S_2})$ where J is the magnetic coupling parameter, g is the average Landé factor and N, β and k have their usual meaning. Least-squares best-fit parameters are: J = -378 cm^{-1} and g = 2.10 for **1** and J = -348 cm^{-1} and g = 2.12 for **2**.

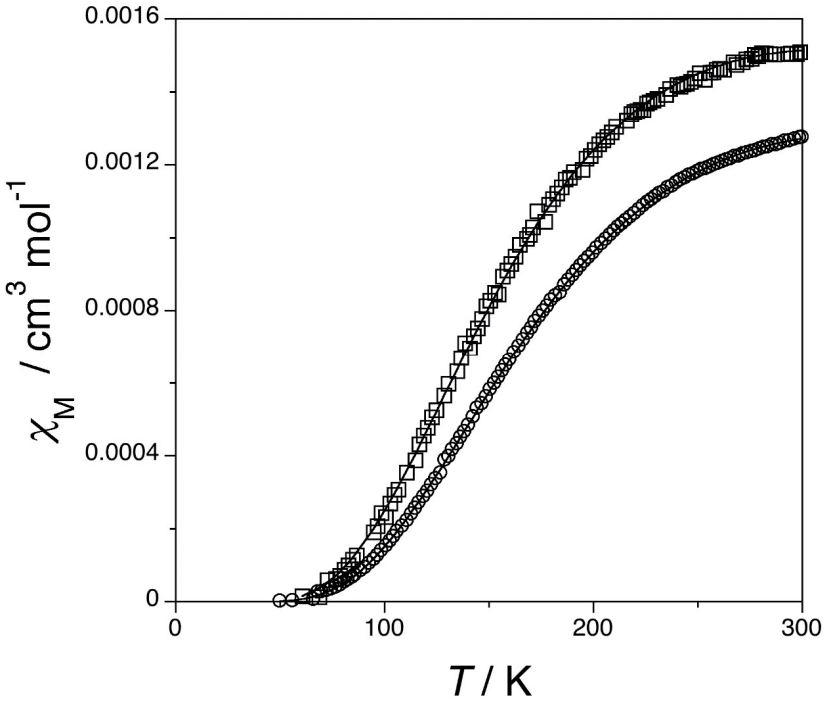

Figure 9. Temperature dependence of χ_M for **1** (○) and **2** (□). The solid lines are the best-fit curves through eq (1) (see text).

The ability of the carboxylato bridge to mediate magnetic interactions between copper(II) ions when acting as a bridge in the *syn-syn* coordination mode accounts for the strong antiferromagnetic couplings in **1** and **2**.[41] The magnitude of the antiferromagnetic interactions in **1** and **2** are somewhat greater than that reported for the well known tetrakis(μ-acetato-*κO:κO'*)bis[(aqua)copper(II)] complex (J = -296 cm^{-1}).[42] This is most likely due to the smaller out-of-plane displacement (h) of the copper(II) ion in **1** and **2** [h = 0.183(2) Å and 0.196(4) Å, respectively] when compared to that in $[Cu_2(CH_3COO)_4(H_2O)_2]$ [h = 0.22(4) Å][43,44] and also to the somewhat shorter copper-

copper separation in the former compounds [ca. 2.60 (**1**) and 2.62 Å (**2**)] against the latter one (ca. 2.64 Å).

The magnetic properties of **3** and **4** in the form of the $\chi_M T$ *vs*. T plots [χ_M being the molar magnetic susceptibility per mononuclear copper(II) unit] are shown in Figure 10. The $\chi_M T$ values of 0.44 (**3**) and 0.46 cm^3 mol^{-1} K (**4**) at room temperature are close to that expected for one magnetically isolated copper(II) ion [$\chi_M T$ = 0.43 cm^3 mol^{-1} K with S_{Cu} = ½ and g = 2.1]. Upon cooling, $\chi_M T$ remains constant up to 50 K for both **3** and **4**, and then it slightly decreases (**3**)/increases (**4**), respectively, reaching $\chi_M T$ values of 0.38 (**3**) and 0.56 cm^3 mol^{-1} K (**4**) at 2.0 K. The different magnetic behavior of **3** and **4** indicates the occurrence of overall weak antiferro- (**3**) and ferromagnetic (**4**) interactions between the copper(II) ions.

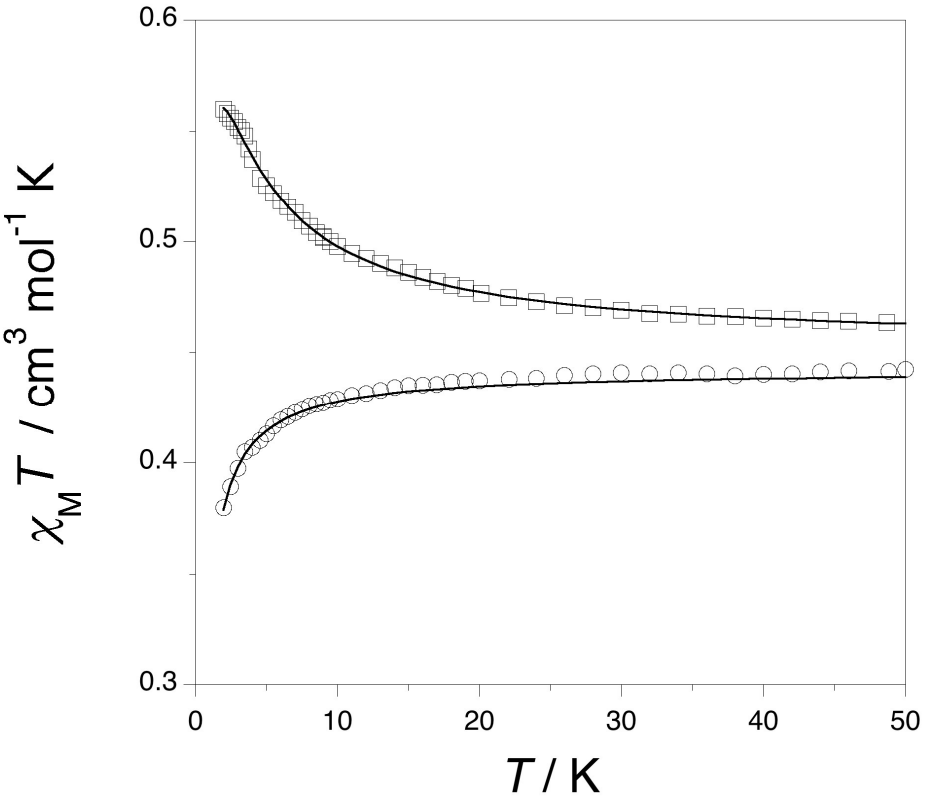

Figure 10. Temperature dependence of $\chi_M T$ for **3** (○) and **4** (□). The solid lines are the best-fit curves through eqns (2) and (1) for compounds **3** and **4**, respectively.

Having in mind that the extended double dps bridges **3** are very poor mediators of magnetic interactions between the copper(II) ions separated by ca. 10.96 Å,[40] a value much shorter than the shortest interchain copper-copper separation (ca. 5.88 Å), we treated the magnetic data of **3** through a Curie-Weiss expression for a mononuclear copper(II) ion [eq (2)]

$$\chi_M = N\beta^2 g^2/4k(T - \theta) \qquad (2)$$

where θ is the Curie-Weiss term. Best-fit parameters are: θ = -0.36 K and g = 2.18.

Dealing with **4**, the observed weak ferromagnetic interaction between the Cu^{II} ions occur within the $[Na^{I}_2Cu^{II}_2(\mu\text{-}O_2CC_8H_9)_4]$ unit, the exchange pathway being provided by di-μ-oxo(carboxylato) which connect the symmetry-related Cu1 and $Cu1^i$ atoms. Consequently, the magnetic data of **4** [per two copper(II) ions] were treated through a Bleaney-Bowers expression for a dicopper(II) unit two interacting copper [eq (1)]. Best-fit results are J = +2.66 cm^{-1} and g = 2.16. The weak ferromagnetic interaction in **4** can be understood on the basis of simple symmetry considerations. The unpaired electron on each copper(II) ion is of the $d(x^2\text{-}y^2)$ type with the x and y axes roughly defined by the short equatorial bonds [mainly located on the $N1N3O1O3^i$ (at Cu1) and $N1^iN3^iO3O1^i$ (at $Cu1^i$) basal planes]. These magnetic orbitals are parallel to each other and they are connected in an equatorial-axial pathway by a double oxo(carboxylate) bridge, the poor overlap between them allowing the prediction of a weak antiferromagnetic interaction which can be ferromagnetic in the case of accidental orthogonality. Well known examples of this out-of-plane exchange pathway concern di-μ-chloro,[45] di-μ-oximato,[46], di-μ-1,1-azido/cyanato[47] and di-μ-oxo(carboxylate) bridged dicopper(II) units (see Table 3), the sign and size of the magnetic interaction depending mainly on the value of the angle at the bridgehead atom (θ) and the basal to apical Cu-X bond distance (R_{ax}). The values of these parameters in the case of **4** are 101.93(9)º and

2.276(3) Å respectively, the ferromagnetic coupling observed corresponding to a case of accidental orthogonality.

Table 3. Selected magneto-structural data for double μ-oxo(carboxylate)-bridged copper(II) complexes

Compound[a]	R_{ax} / Å	θ / ^{o}	J / cm^{-1}	Ref.
{[CuL^1(MeCO$_2$)]$_2$}	2.655(4)	96.3(5)	-1.84	48
{[CuL^2(MeCO$_2$)]$_2$}	2.577(2)	96.1(1)	-1.51	48
{[CuL^3(MeCO$_2$)]$_2$}	2.512(5)	96.9(2)	-1.33	49,50
{[CuL^4(MeCO$_2$)]$_2$·2H$_2$O }$_n$	2.498(8)	98.1(3)	-1.54 (-2.26)[b]	50
{[CuL^5(MeCO$_2$)]$_2$·MeOH }$_n$	2.495(6)	98.3(5)	-1.50 (-7.88)[b]	51
{[CuL^6(MeCO$_2$)]$_2$}·H$_2$O·2 EtOH	2.446(2)	95.7(1)	+0.63[c]	52
	2.651(1)	102.6(1)		
{[Cu(PhCONHCH$_2$CO$_2$)(H$_2$O)$_2$]$_2$}·2H$_2$O	2.37(1)	107.0(5)	-2.15	53,54
{[CuL^7(MeCO$_2$)]$_2$}	2.490(1)	95.34(5)	-0.25	55
{[Cu(tqz)$_2$(HCO$_2$)]$_2$(μ- HCO$_2$)$_2$}·4 H$_2$O	2.331(4)	102.2(2)	-0.52	56
{[Cu(H$_2$O)$_3$][Cu(Phmal)$_2$]}$_n$	2.443(2)	97.38(7)	+1.95[d]	57
{[Cu(bpca)]$_2$(H$_2$opba)}$_2$·6 H$_2$O	2.669(2)	102.81(7)	-2.36	10e
4	2.276(3)	101.93(9)	+2.66	This work

[a]HL^1 = N-(5-Bromosalicylicidene)-N-methylpropane-1,3-diamine, HL^2 = N-methyl-N'-(5-nitrosalicylidene)-propane-1,3-diamine, HL^3 = N-methyl,N'-salicylidenepropane-1,3-diamine, HL^4 = N-methyl-N'-(5-propanesalicylidene)propane-1,3-diamine, HL^5 = N,N'-[bis(2,*o*-hydroxybenzaldeideanimo)-ethyl]ethane-1,2-diamine, HL^6 = N-(2-hydroxy-1,1-dimethylethyl)- salicylideneamine, HL^7 = 7-amino-4-methyl-5-azahept-3-en-2-onate, H2Phmal = phenylmalonic acid, Hbpca = bis(2-pyridylcarbonyl)amide and H$_4$opba = N,N'-1,2-phenilenebis(oxamic) acid. [b]Magnetic analysis through an alternating chain model. [c]This is the only compound whose Cu$_2$O$_2$ core is non-centrosymmetric. [d]This value is *zj* and it has derived from a molecular mean field term.

Finally, the magnetic properties of **5** in the form of the χ_M and $\chi_M T$ *vs.* T plots [χ_M being the molar magnetic susceptibility per two tetracopper(II) units] are shown in Figure 11. $\chi_M T$ at room temperature is 2.84 cm^3 mol^{-1} K, a value which is slightly lower

than that expected for eight magnetically isolated spin doublets ($\chi_M T$ = 3.0 cm^3 mol^{-1} K with S_{Cu} = ½ and g_{Cu} = 2.0). Upon cooling down, $\chi_M T$ continuously decreases and it tends to vanish at low temperatures, while χ_M shows a round maximum at 35 K. These features are characteristic of an overall antiferromagnetic behavior.

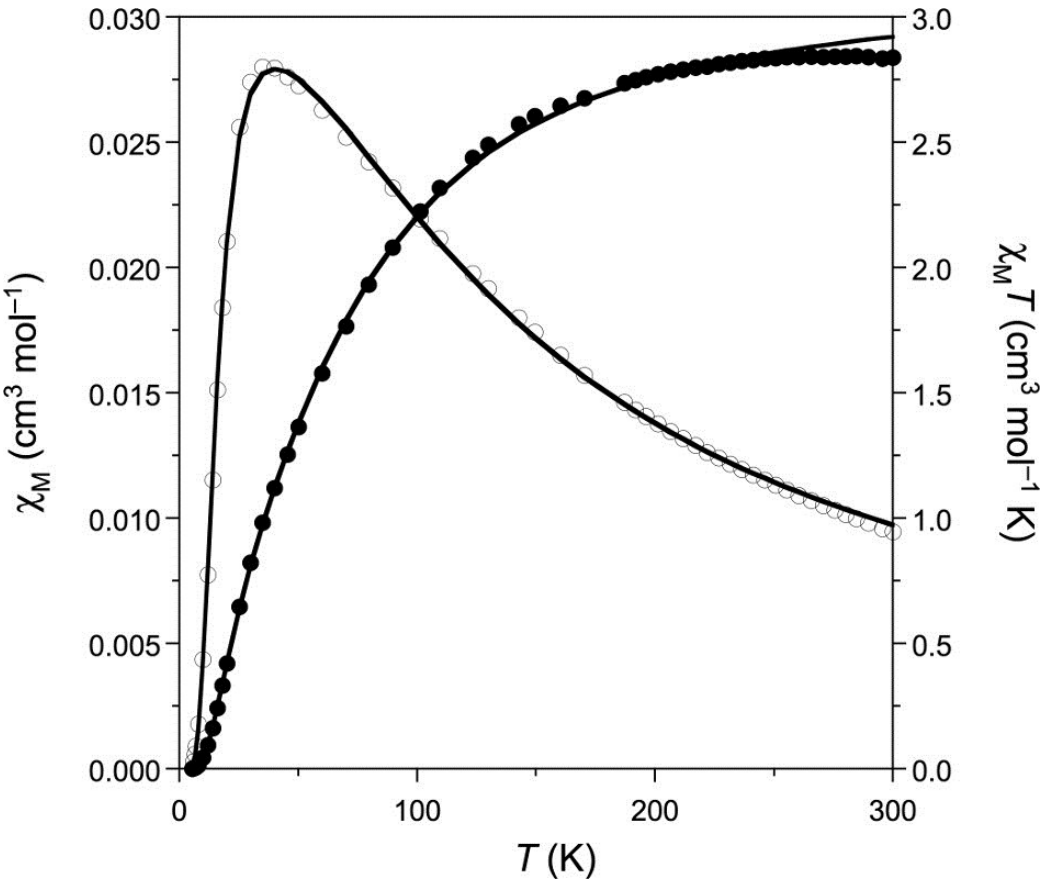

Figure 11. Temperature dependence of $\chi_M T$ (●) and χ_M (○) for **5** under an applied dc field of 5.0 kG. The solid lines are the best-fit curves (see text).

As shown above, two independent tetracopper(II) units, one of them being centrosymmetric (unit 1) and the other non-centrosymmetric (unit 2) are present in **5** and they are interlinked by extended bis-modentate bpp spacers. Assuming that this multiatom spacers are unable to mediate significant magnetic interactions between the copper(II) ions separated by more than 13.6 Å, the magnetic properties of **5** would

correspond to those of the two magnetically non-interaction tetracopper(II) units. Their structural differences makes them non equivalent from a magnetic point of view and given that several exchange pathways coexist in two motifs (see Figure 12), an accurate analysis of the magnetic data is a difficult task. This is why we decided to carry out DFT calculations based on the *broken-symmetry* approach in order to substantiate the efficiency of the different exchange pathways. It deserves to be noted that the calculations of the electronic structure are very sensible to the molecular geometry and the position of the hydrogen atoms of the hydroxo groups in **5** are not well determined, as derived from the very short O–H bond length. Moreover, it has been clearly established that the magnitude and even nature of the magnetic coupling in di-μ-hydroxodicopper(II) complexes is strongly dependent on the position of the hydrogen atom in the hydroxo group.[18a] Thus, the first step in this theoretical study was an optimization of these positions. From these partially optimized geometries (see Tables S1 and S2†), the magnetic coupling constants were estimated for the units 1 and 2 (see Table 4).

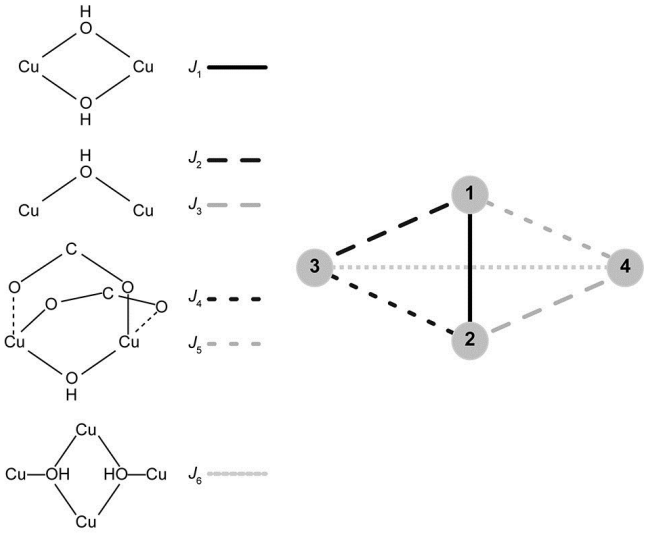

Figure 12. Schematic representation of significant coupling pathways in **5**. The dashed lines in the pictures for the exchange pathways J_4 and J_5 represent long metal-ligand

bonds where the donor atom of the ligand occupy the positions in the Jahn-Teller axis of the copper(II) ion.

Table 4. Calculated J_i constants and selected geometrical parameters for **5**

Pathway[a]	Cu···Cu[b]	θ[c]	τ[d]	J[e]
		Unit 1		
J_1	2.989	99.0 / 99.0	140.5 / 140.5	–132.68(5)
J_2	3.347	117.2	143.9	–32.25(5)
J_3	3.347	117.2	143.9	–32.25(5)
J_4	3.204	111.0	145.5	+39.73(5)
J_5	3.204	111.0	145.5	+39.73(5)
J_6	5.831	---	---	–3.86(5)
		Unit 2		
J_1	2.996	98.9 / 98.4	141.2 / 141.7	–90.2(2)
J_2	3.335	116.5	144.3	–28.2(2)
J_3	3.346	116.9	142.4	–31.7(2)
J_4	3.212	111.0	143.8	+38.5(2)
J_5	3.233	111.5	145.2	+38.2(2)
J_6	5.840	---	---	–7.4(2)

[a]See Figure 12. [b]Copper-copper distances within each tetracopper(II) unit in Å. [c]Values in degrees of the angle at the bridgehead hydroxo. [d]Values in degrees of the angle of the O-H bond with the O···O hydroxo hinge (J_1, J_2, J_3 , J_4, and J_5). [e]Values of the magnetic coupling in cm^{-1}.

In a first attempt where J_6 was not considered, the estimated values of J_i (i = 1-5) exhibited low standard deviations, but they were greater than those usually expected. In fact, J_6 concerns the interaction between 2nd neighbors involving centers 3 and 4 and a pathway constituted by hydroxo groups and the central sites 1 and 2 (see Figure 12). This kind of interaction between centers that are not directly connected has been reported in some cases even with longer exchange pathways.[20] The inclusion of J_6 in the calculations, even though its value being weak, reduces drastically the standard deviation of the J_i values. In order to verify this result and validate its physical meaning, J_6 was also evaluated from DFT calculations on both tetracopper(II) units where two copper(II) ions corresponding to the sites 1 and 2 in Figure 12 were replaced by non-magnetic zinc(II) ions. The values of J_6 that were obtained on these $Cu^{II}_2Zn^{II}_2$ entities [–4.6 cm^{-1} (unit 1) and –8.7 cm^{-1} (unit 2)] were similar to those previously found (see Table 4). On the other hand, the results of the calculations show that, in the two tetracopper(II) units, four J_i constants are organized into pairs (J_2 and J_3 and J_4 and J_5) according to the exchange pathway. This fact is related to the symmetry and the small variations in the structural parameters found in the units 1 and 2, respectively. On the other hand, ferromagnetic couplings are also present even if in agreement with the experimental data, the antiferromagnetic couplings are dominant. Although the strongest magnetic couplings can be organized in three groups, since each carboxylate bridge takes one of the long axial bond of the Cu(II) ion in J_4 and J_5, the hydroxo group is the only operative pathway in all of them. Thus, the J_2 to J_5 set of magnetic couplings can be considered all similar because the two copper(II) ions are connected through one hydroxo group. The very weak differences in the magnitude of antiferro- and ferromagnetic the magnetic coupling within the {J_2 and J_3} and {J_4 and J_5} pairs respectively, are mainly due to non-equal relative positions of the hydrogen atom of the

hydroxo group. In agreement with a previous magneto-structural correlation for di-μ-hydroxodicopper(II) complexes, whereas the $\{J_2, J_3\}$ pair with larger CuOCu (θ) angles is antiferromagnetic, the $\{J_4, J_5\}$ pair is ferromagnetic. This fact leads to the assumption of the existence a value of θ between 111º and 117º for which the magnetic coupling would be null because a transition from ferro- to antiferromagnetic nature would occur. With regard to the known magneto-structural correlation, the value for such a crossing point is too high. However, in contrast to what occurs in the mentioned study, the position of the hydroxo hydrogen in **5** is not free due to the coordination of the hydroxo group to three copper(II) ions. So, instead of the expected values for τ close to 180º in both $\{J_2, J_3\}$ and $\{J_4, J_5\}$ pairs, values about to 140º are found (see Table 4).[18a] On the other hand, according to the presence of two hydroxo ligands as pathway and values of θ greater than the well-known magical angle in the di-μ-hydroxodicopper(II) complexes, a strong antiferromagnetic coupling is found for J_1. These values for the two tetracopper(II) units are similar to those previously found with similar values for θ and τ parameters. Differences between the J_1 values in the units 1 and 2 can be attributed to a sum of changes in the θ and τ angles but also in the Cu-O bond lengths and the γ angle that describes the butterfly distortion of the Cu_2O_2 core.[18]

The simulation of the thermal dependence of the magnetic susceptibility of **5** was performed by using the values of J_i from the DFT calculations as starting parameters. According to these theoretical results, a unique value can be considered for J_2 and J_3 in each tetracopper(II) unit. Thus, this natural simplification can avoid an overparametization in the fitting process. In this way, the isotropic spin Hamiltonian for **5** is given in eq (3)

$$\hat{H} = -\sum_{i=a,b} J_{1i}\hat{S}_{1i}\hat{S}_{2i} + J_{2i}\hat{S}_{1i}\hat{S}_{3i} + J_{3i}\hat{S}_{2i}\hat{S}_{4i} + J_{4i}\hat{S}_{2i}\hat{S}_{3i} + J_{5i}\hat{S}_{1i}\hat{S}_{4i} + J_{6i}\hat{S}_{3i}\hat{S}_{4i} \quad (3)$$

where $J_{2,3} = J_{2a} = J_{2b} = J_{3a} = J_{3b}$ and $J_{4,5} = J_{4a} = J_{4b} = J_{5a} = J_{5b}$. In any case, there are still many parameters and therefore, several possible set of values that are able to reproduce the experimental behavior. However, the set of the best-fit parameters closer to those found from the DFT study that we got are the following: $J_{1a} = -139.8$ cm^{-1}, $J_{1b} = -43.3$ cm^{-1}, $J_{2,3} = -48.1$ cm^{-1}, $J_{4,5} = +58.3$ cm^{-1}, $J_{6a} = -11.2$ cm^{-1}, $J_{6b} = -6.8$ cm^{-1}, $g_{Cu} = 2.05$ and $F = 1.3 \times 10^{-4}$ (F is the agreement factor between the experimental and theoretical data which is defined as $F = \sum[(\chi_M)_{exp} - (\chi_M)_{calcd}]^2/\sum[(\chi_M)_{exp}]^2$). The calculated curves (solid lines in Figure 12) match well the magnetic data in the whole temperature range explored. It deserves to be noted that the magnitude of simulated J_{1b} is smaller than that evaluated by DFT study. In this respect, structural changes as a function of the temperature for hydroxo bridged species can exert a strong influence on the magnetic coupling, specially when these changes concern the angle at the bridgehead hydroxo group. Other set of values close to the theoretically expected can be reached ($J_{1a} = -92.6$ cm^{-1}, $J_{1b} = -74.0$ cm^{-1}, $J_{2,3} = -44.4$ cm^{-1}, $J_{4,5} = +67.4$ cm^{-1}, $J_{6a} = -4.7$ cm^{-1}, $J_{6b} = -12.7$ cm^{-1}, $g_{Cu} = 2.05$ and $F = 7.7 \times 10^{-4}$), but the simulated data do not match so well the experimental data.

Conclusions

Herein, five new copper(II) compounds of formula $[Cu_2(O_2CC_8H_9)_4(pyz)]_n$ (**1**), $[Cu_2(O_2CC_8H_9)_4(dps)]_n$ (**2**), $\{[Cu(O_2CC_8H_9)_2(dps)(H_2O)]\cdot H_2O\}_n$ (**3**), $\{[NaCu(O_2CC_8H_9)_2(bpm)(NO_3)]\cdot H_2O\}_n$ (**4**), and $[Cu_4(O_2CC_8H_9)_6(OH)_2(bpp)_2]_n$ (**5**) have been obtained by diffusion in a first step in a test-shaped glass tube (1.5 cm inner diameter and 18 cm height). We have used the same solvent, room temperature and ratio of the reactants for all complexes, except for **4** where the temperature of the

crystallization was adjusted. Interestingly, **4** constitutes a unique example of heterobimetallic sodium(I)-copper(II) coordination polymer. The magnetic properties of **1**–**5** are governed by the magnetic interactions within the oligonuclear copper(II)-3-phenylpropianate secondary building units (SBUs), the magnetic couplings between the SBUs through the *N*-donor aromatic bridging ligands being negligible in all cases except for **4**. In fact, the extended bis-monodentate dps bridge has revealed to be a very poor mediator of magnetic interactions.[28] The magnetic behavior ranges from a quasi Curie law (**3**) to strong antiferromagnetic (**1** and **2**) or weak ferromagnetic (**4**) coupled Cu^{II}_2 pairs, and coexistence of weak to moderate ferro- and antiferromagnetic interactions in the complex tetracopper(II) units (**5**). In this last case, DFT type calculations were needed to substantiate both the nature and magnitude of the different exchange pathways involved.

Acknowledgements

The authors thank the Conselho Nacional de Desenvolvimento Cientifico e Tecnológico (CNPq), the Fundação de Amparo à Pesquisa do Estado de Minas Gerais (FAPEMIG), the Coordenação de Aperfeiçoamento de Pessoal de Nível Superior (CAPES), FINEP (ref. 134/08), the Brazilian-Spanish Project HB2014-00024, and the Ministerio Español de Ciencia e Innovación (Project CTQ2013-44844P) for financial support. This work is a collaboration research project of members (ACD, FCM and MVM) of the Rede Mineira de Química (RQ-MG) supported by FAPEMIG (Project: CEX - RED-00010-14). The authors and specially Maria Vanda Marinho dedicate this paper to memory of Dr. Wagner Magno Teles.

References

(1) P. Hay, J. C. Thibeault, R. Hoffmannn, *J. Am. Chem. Soc*., 1975, **97**, 4884.

(2) (a) M. V. Marinho, M. I. Yoshida, K. J. Guedes, K. Krambrock, A. J. Bortoluzzi, M. Hörner, F. C. Machado, W. M. Teles, *Inorg. Chem*., 2004, **43**, 1539. (b) M. Melnik *Coord. Chem. Re*v., 1982, **42**, 259; (b) B. Chiari, O. Piovesana, T. Tarantelli, P. F. Zanazzi, *Inorg. Chem.,* 1988, **27**, 3246; (c) D. Kovala-Demertzi, A. Theodorou, M. A. Demertzis, C. P. Raptopoulou, A. Terzis, *J. Inorg. Biochem.,* 1997, **65**, 151.

(3) (a) S. Youngme, A. Cheansirisomboon, C. Danvirutai, C. Pakawatchai, N. Chaichit, *Inorg. Chem. Commun*., 2008, **11**, 57; (b) K. Geetha, A. R. Chakravarty, *J. Chem. Soc., Dalton Trans*., 1999, 1623.

(4) (a) R. Costa, I. P. R. Moreira, S. Youngme, K. Siriwong, N. Wannarit, F. Illas, *Inorg. Chem.,* 2010, **49**, 285; (b) N. Wannarit, K. Siriwong, N. Chaichit, S. Youngme, R. Costa, I. P. R. Moreira, F. Illas, *Inorg. Chem*., 2011, **50**, 10648.

(5) (a) M. C. Dul, E. Pardo, R. Lescouëzec, Y. Journaux, J. Ferrando-Soria, R. Ruiz-García, J. Cano, M. Julve, F. Lloret, D. Cangussu, C. L. M. Pereira, H. O. Stumpf, J. Pasán, C. Ruiz-Pérez, *Coord. Chem. Rev.,* 2010, **254**, 2281; (b) T. Grancha, T. Ferrando-Sorai, M. Castellano, M. Julve, J. Pasán, D. Armentano, E. Pardo, *Chem. Commun.,* 2014, **50**, 7569.

(6) (a) H. Mao, C. Zhang, G. Li, H. Zhang, H. Hou, L. Li, Q. Wu, Y. Zhu, E. Wang *Dalton Trans*., 2004, 3918; (b) A. Rodríguez-Fortea, P. Alemany, S. Alvarez, E. Ruiz, *Chem. Eur. J*., 2001, **7**, 627; (c) J. Boonmak, S. Youngme, N. Chaichit, G. A. van Albada, J. Reedijk, *Cryst. Growth Des*., 2009, ***9***, 3318; (d) E. Colacio, J. M. Domínguez-Vera, M. Ghazi, R. Kivekäs, M. Klinga, J. M. Moreno, *Eur. J. Inorg. Chem.* 1999, 441; (e) S. Youngme, C. Chailuecha, G.A. van Albada, C. Pakawatchai, N.

Chaichit, J. Reedijk, *Inorg. Chim. Acta*, 2005, **358**, 1068; (f) J. Boonmak, S. Youngme, T. Chotkhun, C. Engkagul, N. Chaichit, G. A. van Albada, J. Reedijk, *Inorg. Chem. Commun*., 2008, **11**, 1231; (g) L. Han, Y. Zhou, W.-Na Zhao, X. Li, Y.-X. Liang, *Cryst. Growth Des*., 2009, **9**, 660; (h) D. L. Reger, A. Debreczeni, B. Reinecke, V. Rassolov, M. D. Smith, *Inorg. Chem.* 2009, **48**, 8911.

(7) R. Baggio, R. Calvo, M. T. Garland, O. Peña, M. Perec, L. D. Slep *Inorg. Chem. Commun*., 2007, **10**, 1249.

(8) J. S. Valentine, A. J. Silverstein, Z. *G.* Soos, *J. Am. Chem. Soc*., 1974, **96**, 97.

(9) A. Das, I. Todorov, S. K. Dey, S. Mitra, *Inorg. Chim. Acta*, 2006, **359**, 2041.

(10) (a) P. L. Feng, C. C. Beedle, C. Koo, W. Wernsdorfer, M. Nakano, S. Hill, D. N. Hendrickson, *Inorg. Chem*., 2008, **47**, 3188; (b) L. F. Marques, C, C. Corrêa, H. C. Garcia, T. M. Francisco, S. J. L. Ribeiro, J. D. L. Dutra, R. O. Freire, F. C. Machado, *J. Lumin.* 2014, **148**, 307; (c) T. Manago, S. Hayami, H. Oshio, S. Osaki, H. Hasuyama, R. H. Herber, Y. Maeda, *J. Chem. Soc., Dalton Trans*., 1999, 1001; (d) E. Dubler, U. K. Haring, K. H. Scheller, P. Baltzer, H. Sigel, *Inorg. Chem*., 1984, **23**, 3785; (e) T. R. Simões, R. V. Mambrini, D. O. Reis, M. V. Marinho, M. A. Ribeiro, C. B. Pinheiro, J. Ferrando-Soria, M. Déniz, C. Ruiz-Pérez, D. Cangussu, H. O. Stumpf, F. Lloret, M. Julve, *Dalton Trans.,* 2013, **42**, 5778; (f) L. F. Marques, A. A. B. C. Júnior, C, C. Corrêa, G. Lahoud, R. R. Da Silva, S. J. L. Ribeiro, F. C. Machado, *J. Photochem.Photobiol. A: Chemistry*, 2013, **252**, 69.

(11) M. V. Marinho, M. I. Yoshida, K. Krambrock, L. F. C. De Oliveira, R. Diniz, F. C. Machado*, J. Mol. Struct*., 2009, **923***,* 60.

(12) A. D. Becke, *Phys. Rev. A:At., Mol., Opt. Phys.,* 1968, **38**, 3098; (b) C. T. Lee, W. T. Yang, R. G. Parr, *Phys. Rev. B*, 1988, **37**, 785; (c) A. D. Becke, *J. Chem. Phys.,* 1993, **98**, 5648.

(13) M. J. Frisch, *et al.*, Gaussian 09, (Rev. D01); Gaussian, Inc., Wallingford, CT, 2009.

(14) A. Schafer, H. Horn, R. Ahlrichs, *J. Chem. Phys.,* 1992, **97**, 2571.

(15) A. Schaefer, C. Huber, R. Ahlrichs, *J. Chem. Phys.,* 1994, **100**, 5829.

(16) J. Tomasi, B. Mennucci, R. Cammi, *Chem. Rev.,* 2005, **105**, 2999.

(17) D. Visinescu, L. M. Toma, O. Cano, O. Fabelo, C. Ruiz-Pérez, A. Labrador, F. Lloret, M. Julve, *Dalton Trans.,* 2010, **39**, 5028.

(18) (a) E. Ruiz, P. Alemany, S. Alvarez, J. Cano, *J. Am. Chem. Soc.,* 1997, **119**, 1297; (b) E. Ruiz, P. Alemany, S. Alvarez, J. Cano, *Inorg. Chem.* 1997, **36**, 3683.

(19) E. Ruiz, J. Cano, S. Alvarez, P. Alemany , *J. Comp. Chem.,* 1999, **20**, 1391.

(20) E. Ruiz, A. Rodríguez-Fortea, J. Cano, S. Alvarez, P. Alemany, *J. Comp. Chem.*, 2003, **24**, 982.

(21) E. Ruiz, S. Alvarez, J. Cano, V. Polo, *J. Chem. Phys.,* 2005, **123**, 164110.

(22) Xcalibur CCD system, Agilent Technologies: *CrysAlisPro Software system*, version 1.171.35.15, Agilent Technologies UK Ltd, Oxford, 2011.

(23) (a) XPREP Version 2013/3 (Sheldrick, Bruker AXS Inc.); (b) G. M. Sheldrick (XS Version 2013/1), *Acta Crystallogr*. 2008, **A64**, 112; (c) G. M. Sheldrick (XL Version 2013/3), *Acta Crystallogr*. 2008, **A64**, 112

(24) SAINT Version 8.34A (Bruker AXS Inc., 2013).

(25) SADABS Version 2012/1 (Sheldrick, Bruker AXS Inc.).

(26) L. Palatinusz, G. Chapuis, *J. Appl. Crystallogr.* 2007, **40**, 786.

(27) G .M. Sheldrick, *Acta Crystallogr*. 2008, **A64**, 112.

(28) C. K. Johnson, *Crystallographic Computing*, Ahmed, F. R., Ed.; S. R. Hall & C. P. Huber. Copenhagen: Munksgaard. 1970, 207.

(29) F. L. Hirshfeld, *Acta Crystallogr*., 1976, **A32**, 239.

(30) D. Braga, T.F. Koetzle, *Acta Crystallogr*. 1988, **B44**, 151.

(31) Platon: A. L. Spek, *Acta Crystallogr*. 2009, **D65**, 148.

(32) (a) K. Brandenburg, H. Putz *DIAMOND 2.1d*; Crystal Impact: Bonn, Germany, 2000; (b) F. Macrae, P. R. Edgington, P. McCabe, E. Pidcock, G. P. Shields, R. Taylor, M. Towler; Streek van der, J. J. *Appl. Crystallogr*. 2006, **39**, 453.

(33) C. K. Johnson, *In Crystallographic Computing*, F. R. Ahmed, Ed.; Copenhagen, Denmark, 1970, 217.

(34) J.-P. Zhao, S.-D. Han, R. Zhao, Q. Yang, Z. Chang, X.-D. Bu, *Inorg. Chem*., 2013, **52**, 2862.

(35) (a) G. B. Deacon, R. J. Phillips, *Coord. Chem. Rev.,* 1980, **33**, 227. (b) K. Nakamoto, *Infrared and Raman Spectra of Inorganic and Coordination Compounds*, 4th ed.; Wiley: New York, 1986.

(36) G. De Munno, D. Armentano, M. Julve, F. Lloret, R. Lescouëzec, J. Faus, *Inorg. Chem.,* 1999, **38**, 2234.

(37) N. Marino, D. Armentano, G. De Munno, J. Cano, F. Lloret, M. Julve, *Inorg. Chem*. 2012, **51**, 4323.

(38) The trigonality index τ (τ = 0 and 1 for ideal square pyramidal and trigonal bipyramidal environments, respectively) was calculated as specified in A. W. Addison, T. N. Rao, J. Reedijk, J. van Rijn, G. C. Verschoor, *J. Chem. Soc., Dalton Trans*., 1984, 1349.

(39) A. B. Caballero, C. Marín, I. Ramírez-Macias, A. Rodríguez-Diéguez, M. Quirós, J. M. Salas, M. Sánchez-Moreno, *Polyhedron*, 2012, **33**, 137.

(40) M. V. Marinho, L. F. Marques, R. Diniz, H. O. Stumpf, L. C. Visentin, M. I. Yoshida, F. C. Machado, F. Lloret, M. Julve, *Polyhedron*, 2012, **45**, 1.

(41) (a) A. Rodríguez-Fortea, P. Alemany, S. Alvarez, R. Ruiz, *Chem. Eur. J.,* 2001, **7**, 627; (b) S. Dali, P. S. Mukherjee, E. Zangrando, F. Lloret, N. R. Chaudhuri, *J. Chem. Soc., Dalton Trans.*, 2000, 822; (c) A. Das, I. Todorov, S. K. Dey, S. Mitra, *Inorg. Chim. Acta*, 2006, **359**, 2041; (d) C. Yuste-Vivas, M. R. Silva, P. Martín-Ramos, L. J. C. Pereira, J. Ferrando-Soria, P. Amorós, M. Julve, *Polyhedron*, 2015, **87**, 220.

(42) O. Kahn, Molecular Magnetism, VCH Publishers Inc., 1993.

(43) J. N. Van Niekerk, F. R. L. Schoening, *Nature*, 1953, **171**, 36.

(44) J. N. Van Niekerk, F. R. L. Schoening, *Acta Crystallogr.*, 1951, **4**, 35.

(45) (a) M. Hernández-Molina, J. González-Platas, C. Ruiz-Pérez, F. Lloret, M. Julve, *Inorg. Chim. Acta*, 1999, **284**, 258; (b) H. Grove, J. Sletten, M. Julve, F. Lloret, *J. Chem. Soc., Dalton Trans.*, 2001, 2487; (c) S. Mandal, F. Lloret, R. Mukherjee, *Inorg. Chim. Acta*, 2009, **362**, 27.

(46) B. Cervera, R. Ruiz, F. Lloret, M. Julve, J. Cano, J. Faus, C. Bois, J. Mrozinski, *J. Chem. Soc., Dalton Trans.,* 1997, 395.

(47) (a) G. De Munno, M. G. Lombardi; M. Julve, F. Lloret, J. Faus, *Inorg. Chim. Acta*, 1998, **282**, 82; (b) J. Carranza, J. Sletten, F. Lloret, *J. Mol. Struct.,* 2008, **890**, 31; (c) C. Adhikary, S. Koner, *Coord. Chem. Rev.,* 2010, **254**, 2933.

(48) B. Chiari, J. H. Helms, O. Piovesana, T. Tarantelli, P. F. Zanazzi, *Inorg. Chem.,* 1986, **25**, 2408.

(49) R. Hämäläinen; M. Ahlgren, U. Turpeinen, *Acta Crystallogr., Sect. B: Struct. Crystallogr. Cryst. Chem.,* 1982, **38***,* 1577.

(50) B. Chiari, J. H. Helms, O. Piovesana, T. Tarantelli, P. F. Zanazzi, *Inorg. Chem.,* 1986, **25**, 870.

(51) B. Chiari, W. F. Hatfield, O. Piovesana, T. Tarantelli, P. F. Zanazzi, *Inorg. Chem.*, 1983, **22**, 1468.

(52) A. M. Greenaway, C. J. O'Connor, J. W. Overman, E. Sinn, *Inorg. Chem.,* 1981, **20**, 1508.

(53) J. M. Brown, L. M. Trefonas, *Inorg. Chem.,* 1973, **312**, 1730.

(54) E. Dixon-Estes, E. F. Estes, R. P. N. Scaringe, W. E. Hatfield, D. J. Hodgson, *Inorg. Chem.,* 1975, **14**, 2564.

(55) J. P. Costes, F. Dahan, J. P. Laurent, *Inorg. Chem.,* 1985, **24**, 1018.

(56) E. Escrivá, J. Server-Carrió, L. Lezama, J. V. Folgado, J. L. Pizarro, R. Ballesteros, B. Abarca, *J. Chem. Soc., Dalton Trans.,* 1997, 2033.

(57) J. Pasán, J. Sanchiz, C. Ruiz.Pérez, F. Lloret, M. Julve, *New J. Chem.,* 2003, **27**, 1557.